

Differentially Private Fisher Randomization Tests for Binary Outcomes

Qingyang Sun*

Department of Statistical Science, Duke University

and

Jerome P. Reiter

Department of Statistical Science, Duke University

December 16, 2025

Abstract

Across many disciplines, causal inference often relies on randomized experiments with binary outcomes. In such experiments, the Fisher randomization test provides exact, assumption-free tests for causal effects. Sometimes the outcomes are sensitive and must be kept confidential, for example, when they comprise physical or mental health measurements. Releasing test statistics or p -values computed with the confidential outcomes can leak information about the individuals in the study. Those responsible for sharing the analysis results may wish to bound this information leakage, which they can do by ensuring the released outputs satisfy differential privacy. In this article, we develop several differentially private versions of the Fisher randomization test for binary outcomes. Specifically, we consider direct perturbation approaches that inject calibrated noise into test statistics or p -values, as well as a mechanism-aware, Bayesian denoising framework that explicitly models the privacy mechanism. We further develop decision-making procedures under privacy constraints, including a Bayes risk-optimal rule and a frequentist-calibrated significance test. Through theoretical results, simulation studies, and an application to the ADAPTABLE clinical trial, we demonstrate that our methods can achieve valid and interpretable causal inference while ensuring the differential privacy guarantee.

Keywords: Confidentiality; Decision; Experiment; Hypothesis; Privacy.

*The authors gratefully acknowledge funding from grant NSF-SES-2217456.

1 Introduction

Randomization-based inference is a cornerstone of causal analysis, offering inferences that derive solely from the randomization of treatment assignments to study subjects. Among such methods, the Fisher randomization test (FRT) is one of the most widely used approaches (Fisher 1935). In the FRT, one presumes Fisher’s sharp null hypothesis: each individual’s outcome is the same regardless of treatment assignment. Under this sharp null, one can use the observed outcomes to compute the value of the chosen test statistic for any possible randomization and thereby construct a reference distribution for the test statistic. The analyst compares the observed value of the test statistic to this reference distribution, resulting in a p -value under the null hypothesis. In this article, we consider FRTs for binary outcomes in completely randomized experiments.

In many causal studies, the binary outcomes are inherently sensitive, such as indicators of a disease or a risky behavior, and therefore should be kept confidential. The literature on data privacy has shown that releasing results of any statistical analysis leaks information about the underlying study subjects. Even releasing summary statistics can introduce disclosure risks (Dinur & Nissim 2003, Dwork et al. 2017, Abowd et al. 2022). Thus, those responsible for sharing the analysis results of a FRT with confidential outcomes may want to limit the amount of information leakage.

One way to bound this leakage is to ensure the released results satisfy differential privacy (DP) (Dwork 2006, Dwork et al. 2006), which offers a rigorous privacy guarantee. While researchers have developed DP methods for causal inference (e.g., D’Orazio et al. 2015, Lee et al. 2019, Niu et al. 2022, Mukherjee et al. 2024, Guha & Reiter 2025) and for hypothesis testing (e.g., Gaboardi et al. 2016, Couch et al. 2019, Awan & Slavković 2018, Kazan et al. 2023, Kalemaj et al. 2024, Peña & Barrientos 2025), to our knowledge, there do not exist DP algorithms for FRTs.

We aim to close that gap by developing differentially private Fisher randomization tests for binary outcomes, which we abbreviate as DP-FRTs. We explore direct perturbation mechanisms that add calibrated noise to the p -value or test statistic. We also propose a mechanism-aware, Bayesian denoising approach that explicitly models the DP noise to recover a posterior distribution for the confidential p -value. We develop decision frameworks under both Bayesian and frequentist paradigms that translate privatized p -values into actionable conclusions. In the Bayesian framework, we include an option for analysts to abstain from making a decision when the evidence is inconclusive, then refine or update their conclusions by spending additional privacy budget. In the frequentist-calibrated framework, we control type I error rates, ensuring that privacy protection does not compromise the nominal significance level. Together, these frameworks enable reliable and interpretable causal conclusions with formal privacy guarantees.

The remainder of this article is organized as follows. Section 2 reviews the FRT for binary outcomes and key concepts of DP. Section 3 presents the DP-FRTs, including the direct perturbation and Bayesian denoising methods. Section 4 describes the Bayesian and frequentist decision-making frameworks. Section 5 presents simulation studies and a genuine data analysis that assess the performance of the proposed methods and offer guidance for their implementation. Section 6 concludes with a discussion and potential extensions. Proofs of lemmas and theorems are provided in the supplementary material.

2 Background

In Section 2.1, we review the FRT in the context of completely randomized experiments with binary outcomes. In Section 2.2, we review key concepts and properties of DP.

2.1 Fisher Randomization Test for Binary Outcomes

We develop DP-FRTs under the potential outcomes framework for causal inference (Rubin 1974). For each unit $i = 1, \dots, n$ in the study, let $Z_i = 1$ when unit i is assigned to treatment and $Z_i = 0$ when the unit is assigned to control. For $i = 1, \dots, n$, let $Y_i(1)$ and $Y_i(0)$ be the outcomes for unit i under treatment and control, respectively. Under the stable unit treatment value assumption, the observed outcome is $Y_i^{\text{obs}} = Z_i Y_i(1) + (1 - Z_i) Y_i(0)$.

The full collection $\{(Y_i(1), Y_i(0))\}_{i=1}^n$ is often referred to as the ‘‘Science,’’ which represents the underlying object of interest in causal inference. The Science is never fully observed, since only one of $(Y_i(1), Y_i(0))$ is realized for each unit i . Let n_{11} and n_{10} be the numbers of treated units with $Y_i^{\text{obs}} = 1$ and $Y_i^{\text{obs}} = 0$, respectively. Let n_{01} and n_{00} be the corresponding counts in the control group. Let n_1 and n_0 be the sizes of the treatment and control groups, and n_{+1} and n_{+0} be the marginal counts of each outcome.

Fisher (1935) proposed to test the null hypothesis of no individual causal effects, that is, $H_0^{\text{F}} : Y_i(1) = Y_i(0)$ for $i = 1, \dots, n$. For completely randomized experiments (CRE), the FRT under H_0^{F} proceeds as follows. Let $\mathbf{Z} = (Z_1, \dots, Z_n)$ be the vector of treatment assignments, with \mathbf{Z}^{obs} the realized assignment. Let $\mathbf{Y}^{\text{obs}} = (Y_1^{\text{obs}}, \dots, Y_n^{\text{obs}})$ be the vector of observed outcomes. First, the analyst selects a test statistic $T(\mathbf{Z}; \mathbf{Y}^{\text{obs}})$ that reflects deviations from H_0^{F} . The value of the observed statistic is $T^{\text{obs}} = T(\mathbf{Z}^{\text{obs}}; \mathbf{Y}^{\text{obs}})$. Under the known assignment mechanism of CRE, the analyst evaluates $T(\mathbf{Z}; \mathbf{Y}^{\text{obs}})$ for each possible randomization \mathbf{Z} that adheres to the design to obtain the randomization distribution under H_0^{F} . The (one-sided) FRT p -value is

$$p_{\text{FRT}} = \Pr\left(T(\mathbf{Z}; \mathbf{Y}^{\text{obs}}) \geq T^{\text{obs}}\right) = \frac{1}{|\mathcal{Z}|} \sum_{\mathbf{Z} \in \mathcal{Z}} \mathbf{1}(T(\mathbf{Z}; \mathbf{Y}^{\text{obs}}) \geq T^{\text{obs}}), \quad (1)$$

where $|\mathcal{Z}|$ is the total number of possible random assignments. When $|\mathcal{Z}|$ is large, one can approximate p_{FRT} using Monte Carlo methods.

For binary outcomes, a natural choice of the test statistic is the difference in sample proportions, $\hat{\tau} = n_{11}/n_1 - n_{01}/n_0$. In this case, the FRT coincides numerically with Fisher’s exact test for 2×2 tables. That is, under H_0^F , n_{11} follows a hypergeometric distribution so that, for $a = \max\{0, n_1 - n_{+0}\}, \dots, \min\{n_1, n_{+1}\}$, we have

$$n_{11} \sim \text{Hypergeometric}(n, n_{+1}, n_1), \quad \Pr(n_{11} = a) = \frac{\binom{n_{+1}}{a} \binom{n_{+0}}{n_1 - a}}{\binom{n}{n_1}}. \quad (2)$$

2.2 Differential Privacy

In DP, we view a data-release procedure as a randomized algorithm \mathcal{M} that takes a dataset D as input and produces a randomized output. The privacy guarantee is defined with respect to neighboring datasets, i.e., datasets that differ in the data of a single individual, such as by adding, removing, or modifying one record. DP requires that the output distributions produced by \mathcal{M} on any pair of neighboring datasets be nearly indistinguishable. Consequently, it becomes difficult for an adversary to determine whether a specific individual is present in the dataset or to infer sensitive attributes with high confidence.

Definition 2.1. A randomized algorithm \mathcal{M} satisfies ϵ -differential privacy (ϵ -DP) if, for any pair of neighboring datasets D and D' and for all measurable subsets $S \subseteq \mathcal{R}(\mathcal{M})$,

$$\Pr(\mathcal{M}(D) \in S) \leq e^\epsilon \Pr(\mathcal{M}(D') \in S). \quad (3)$$

The privacy parameter $\epsilon > 0$ is referred to as the privacy budget. Smaller values of ϵ provide stronger privacy guarantees; however, they also typically result in greater perturbations to the results computed with the confidential data. The literature on DP suggests values of $\epsilon < 1$ to provide robust privacy guarantees, although larger values often are used in practical applications (Kazan & Reiter 2024b).

We make use of three properties of DP when designing the private FRT algorithms. The first is post-processing invariance. If \mathcal{M} is an ϵ -DP mechanism and g is any (possibly

randomized) function that does not depend on the data, then $g \circ \mathcal{M}$ also satisfies ϵ -DP. The second is sequential composition. Suppose \mathcal{M}_1 satisfies ϵ_1 -DP and \mathcal{M}_2 satisfies ϵ_2 -DP. Then, the joint release of $(\mathcal{M}_1(D), \mathcal{M}_2(D))$ satisfies $(\epsilon_1 + \epsilon_2)$ -DP. The third is parallel composition. If \mathcal{M}_1 and \mathcal{M}_2 are applied to disjoint subsets of data, then the overall mechanism satisfies $\max(\epsilon_1, \epsilon_2)$ -DP.

To ensure DP, a typical approach is to add random noise calibrated to the sensitivity of the released quantity. Let $f : \mathcal{D} \rightarrow \mathbb{R}^d$ be a function defined on datasets. The ℓ_1 -sensitivity of f is defined as $\Delta f = \max_{D, D'} \|f(D) - f(D')\|_1$, where the maximum is taken over all pairs of neighboring datasets D and D' . For example, when $f(D)$ produces a count, $\Delta f = 1$.

A common ϵ -DP mechanism used in continuous domains is the Laplace mechanism (Dwork 2006). The Laplace mechanism releases $\tilde{f}(D) = f(D) + \eta$, where $\eta \sim \text{Lap}(0, \Delta f / \epsilon)$ with $p_\eta(h) = (\epsilon / (2\Delta f)) \exp(-\epsilon|h| / \Delta f)$. Another common mechanism, particularly for count data, is the Geometric mechanism (Ghosh et al. 2012). Let $\rho = \exp(-\epsilon / \Delta f)$. The Geometric mechanism releases $\tilde{f}(D) = f(D) + \eta$ where $\eta \sim \text{Geom}(\rho)$ with $\Pr(\eta = h) = ((1 - \rho) / (1 + \rho)) \rho^{|h|}$, where $h \in \mathbb{Z}$. We use both the Laplace and Geometric mechanisms in the DP-FRT algorithms.

3 DP Estimation of the FRT p -value

This section presents ϵ -DP approaches for privatizing the FRT p -value, including the direct perturbation methods (Section 3.1) and the Bayesian denoising framework (Section 3.2). For both approaches, to define the DP guarantee we consider neighboring databases as two study populations that differ in one individual but receive the same treatment assignments. This presumes (n_1, n_0) and \mathbf{Z}^{obs} are fixed by the design of CRE and are public knowledge.

3.1 Direct Perturbation Approaches

One approach is to directly perturb the exact p -value using a Laplace mechanism. Lemma 3.1 provides the sensitivity of p_{FRT} .

Lemma 3.1. *Under the CRE with binary outcomes and the test statistic $\hat{\tau}$, the ℓ_1 -sensitivity of p_{FRT} is $\Delta_p = \max\{n_1/n, n_0/n\}$.*

Based on Lemma 3.1, we can release privatized FRT p -values by adding Laplace noise calibrated to the sensitivity and clipping to the feasible range. Define $[L, U] = [|\mathcal{Z}|^{-1}, 1]$. We release $\tilde{p} = \Pi_{[L,U]}(p_{\text{FRT}} + \eta)$, where $\eta \sim \text{Lap}(0, \Delta_p/\epsilon)$ and $\Pi_{[L,U]}(x) = \min\{U, \max\{L, x\}\}$ is the clipping operator. We call this method DP-FRT-p. Theorem 3.2 states the privacy guarantee for DP-FRT-p, which follows from the Laplace mechanism and the post-processing invariance of DP. The latter ensures that clipping does not degrade privacy.

Theorem 3.2. *For fixed ϵ , \tilde{p} produced by DP-FRT-p satisfies ϵ -DP.*

Another alternative is to perturb the test statistic and pair it with a privatized randomization distribution. Lemma 3.3 provides the ℓ_1 -sensitivity of $\hat{\tau} = n_{11}/n_1 - n_{01}/n_0$.

Lemma 3.3. *Under the CRE with binary outcomes, the ℓ_1 -sensitivity of $\hat{\tau}$ is $\Delta_{\hat{\tau}} = \max\{1/n_1, 1/n_0\}$.*

To implement this approach, we separately perturb the observed test statistic and its randomization distribution. Privatizing the randomization distribution is necessary since it depends on the total number of observed successes n_{+1} , which is computed from the confidential data. Based on Lemma 3.3, we first release $\tilde{T}^{\text{obs}} = \Pi_{[-1,1]}(\hat{\tau} + \eta_{\text{obs}})$ with $\eta_{\text{obs}} \sim \text{Lap}(0, \Delta_{\hat{\tau}}/\epsilon_{\text{obs}})$. We then release $\tilde{n}_{+1} = \Pi_{\{0,1,\dots,n\}}(n_{+1} + \eta_{\text{ref}})$ with $\eta_{\text{ref}} \sim \text{Geom}(\exp(-\epsilon_{\text{ref}}))$. As a default, we set $\epsilon_{\text{obs}} = \epsilon_{\text{ref}} = \epsilon/2$, where ϵ is the total privacy budget. Given $(\tilde{T}^{\text{obs}}, \tilde{n}_{+1})$, we compute the privatized Fisher tail probability $\tilde{p} = \Pr(\tilde{n}_{11}/n_1 - (\tilde{n}_{+1} - \tilde{n}_{11})/n_0 \geq \tilde{T}^{\text{obs}})$ for $\tilde{n}_{11} \sim \text{Hypergeometric}(n, \tilde{n}_{+1}, n_1)$. We refer to this procedure as DP-FRT-t. The privacy

guarantee is stated in Theorem 3.4. It follows from the properties of the Laplace mechanism, the Geometric mechanism, and the post-processing invariance of DP.

Theorem 3.4. *For fixed $\epsilon = \epsilon_{\text{obs}} + \epsilon_{\text{ref}}$, \tilde{p} produced by DP-FRT-t satisfies ϵ -DP.*

The direct perturbation approaches have some limitations. First, for DP-FRT-p, the addition of DP noise can strongly distort the FRT p -value. Per Lemma 3.1, the sensitivity of p_{FRT} is at least $1/2$, which is substantial relative to $[0, 1]$. Moreover, clipping outputs can introduce bias. Second, \tilde{p} may not retain the properties of a valid p -value. For example, \tilde{p} is no longer guaranteed to satisfy $\Pr(\tilde{p} \leq \alpha) \leq \alpha$ under H_0^F for any prespecified level $\alpha \in [0, 1]$. Third, DP-FRT-p and DP-FRT-t do not provide uncertainty quantification for the privatized outputs. The absence of uncertainty measures limits the interpretability and transparency of the results. Simulation studies illustrating the unsatisfactory performance of DP-FRT-p and DP-FRT-t are provided in the supplementary material.

3.2 FRT via Bayesian Denoising

The shortcomings of the methods in Section 3.1 motivate us to develop a Bayesian denoising approach that explicitly accounts for the DP mechanism. The overarching strategy is to privatize the sufficient statistics, update a Bayesian model for the underlying true counts, and map the posterior distribution onto the space of p -values. The resulting posterior distribution for p_{FRT} is the DP release. We call this approach DP-FRT-Bayes. The algorithm begins by adding noise to $(n_{11}, n_{10}, n_{01}, n_{00})$. Since (n_1, n_0) are fixed by design, it suffices to privatize n_{11} and n_{01} . Specifically, given ϵ , we perturb (n_{11}, n_{01}) by

$$\tilde{\mathbf{n}} = (\tilde{n}_{11}, \tilde{n}_{01}) = (n_{11} + \eta_{11}, n_{01} + \eta_{01}), \quad \eta_{11}, \eta_{01} \stackrel{\text{i.i.d.}}{\sim} \text{Geom}(\exp(-\epsilon)). \quad (4)$$

Modifying the outcome of a single individual only changes the success count within that individual's assigned group. Consequently, at most one of n_{11} or n_{01} can change by ± 1 . Therefore, the ℓ_1 -sensitivity of the pair (n_{11}, n_{01}) is one.

To describe the post-processing Bayesian inference, we introduce (m_{11}, m_{01}) as random variables for (n_{11}, n_{01}) , which are unknown to the analyst who has the DP noisy counts $\tilde{\mathbf{n}}$. We specify a data-independent prior π on (m_{11}, m_{01}) with support $\{0, \dots, n_1\} \times \{0, \dots, n_0\}$. The posterior distribution is then $\Pr(m_{11} = a, m_{01} = b \mid \tilde{\mathbf{n}}) \propto w(a, b)$, where $w(a, b) = \pi(a, b)\kappa_\rho(\tilde{n}_{11} - a)\kappa_\rho(\tilde{n}_{01} - b)$. Here, $\kappa_\rho(h) = ((1 - \rho)/(1 + \rho))\rho^{|h|}$ is the two-sided geometric kernel with $\rho = \exp(-\epsilon)$.

For each candidate pair of true counts (a, b) , let $K = a + b$ denote the corresponding total number of observed successes. Under the sharp null H_0^F and using (2), the one-sided FRT p -value corresponding to (a, b) is given by:

$$p_{ab} = \sum_{t=\max\{a, K-n_0\}}^{\min(n_1, K)} \frac{\binom{K}{t} \binom{n-K}{n_1-t}}{\binom{n}{n_1}}. \quad (5)$$

Denote $\gamma(a, b) = \Pr(m_{11} = a, m_{01} = b \mid \tilde{\mathbf{n}})$. The deterministic mapping $(a, b) \mapsto p_{ab}$ induces the following posterior distribution of p_{FRT} given $(\tilde{n}_{11}, \tilde{n}_{01})$:

$$\Pr(p_{\text{FRT}} \in B \mid \tilde{\mathbf{n}}) = \sum_{a=0}^{n_1} \sum_{b=0}^{n_0} \gamma(a, b) \mathbf{1}(p_{ab} \in B), \quad B \subseteq [0, 1]. \quad (6)$$

Note that using DP-FRT-Bayes allows \tilde{n}_{11} and \tilde{n}_{01} to fall outside $[0, n_1]$ or $[0, n_0]$, respectively. Clipping the DP counts to the feasible range is not necessary, as the posterior distribution enforces the constraints automatically. Further, as shown in the supplementary material, under the Geometric mechanism posterior inferences are identical regardless of whether or not the DP counts are clipped.

By the Geometric mechanism, the release of $(\tilde{n}_{11}, \tilde{n}_{01})$ satisfies ϵ -DP. Since all later steps use post-processing, DP-FRT-Bayes satisfies ϵ -DP, as formally stated in Theorem 3.5.

Theorem 3.5. $\Pr(p_{\text{FRT}} \mid \tilde{\mathbf{n}})$ released by DP-FRT-Bayes satisfies ϵ -DP.

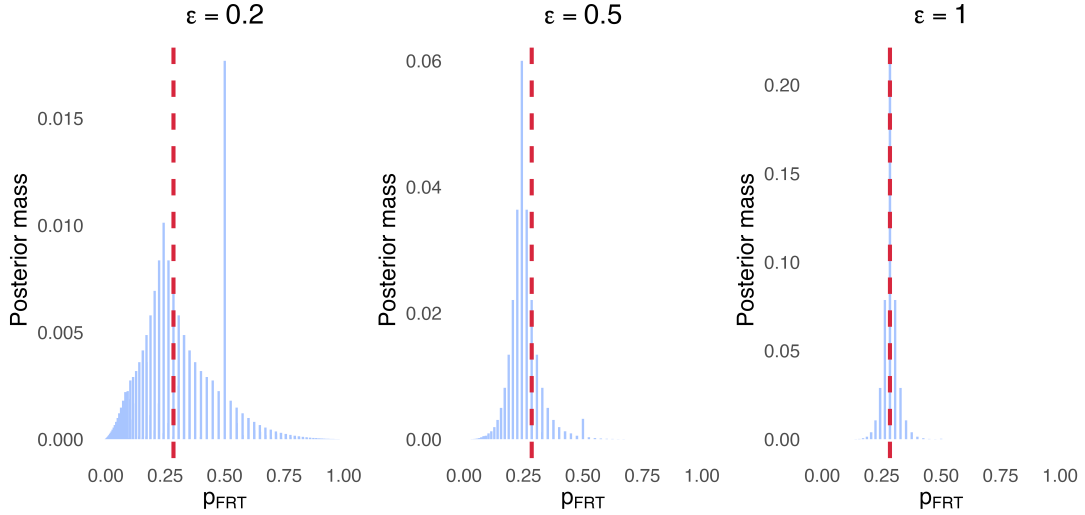


Figure 1: Posterior distributions from DP-FRT-Bayes under $\epsilon \in \{0.2, 0.5, 1\}$. The red dashed line indicates the non-private p -value, which equals 0.2846.

To provide an illustrative example of DP-FRT-Bayes, we consider data with $n_1 = n_0 = 500$, $n_{11} = 260$, and $n_{01} = 250$. We use a two-dimensional discrete uniform prior on (m_{11}, m_{01}) . Figure 1 shows the posterior probability mass functions when $\epsilon \in \{0.2, 0.5, 1\}$. When ϵ is small, the posterior is highly diffuse and exhibits a mode at $p_{\text{FRT}} = 0.5$, reflecting greater uncertainty due to the DP noise. As ϵ increases, the posterior concentrates more sharply around the non-private value.

3.2.1 Prior Specification for Counts

While conceptually analysts can posit any prior distribution for (m_{11}, m_{01}) for the Bayesian denoising, it is well known in DP that informative prior distributions can have a strong influence on the posterior (Kazan & Reiter 2024a). Therefore, we expect many analysts will prefer to use default prior distributions with DP-FRT-Bayes. A natural choice is the discrete uniform prior,

$$\pi_{\text{unif}}(a, b) = \frac{1}{(n_1 + 1)(n_0 + 1)}, \quad a \in \{0, \dots, n_1\}, b \in \{0, \dots, n_0\}. \quad (7)$$

This choice facilitates computations and avoids privileging any specific configuration between the treatment and the control groups.

Another option arises from the independent binomial formulation commonly used in clinical practice. Specifically, we independently posit $m_{11} \sim \text{Binom}(n_1, p_1)$ and $m_{01} \sim \text{Binom}(n_0, p_0)$, together with independent priors $p_1 \sim \text{Beta}(\alpha_1, \beta_1)$ and $p_0 \sim \text{Beta}(\alpha_0, \beta_0)$. Integrating out (p_1, p_0) yields the independent Beta-binomial prior for the counts,

$$\pi_{\text{BB}}(a, b; \alpha_1, \beta_1, \alpha_0, \beta_0) = \frac{\binom{n_1}{a} B(a + \alpha_1, n_1 - a + \beta_1) \binom{n_0}{b} B(b + \alpha_0, n_0 - b + \beta_0)}{B(\alpha_1, \beta_1) B(\alpha_0, \beta_0)}, \quad (8)$$

where the Beta function $B(x, y) = \Gamma(x)\Gamma(y)/\Gamma(x + y)$. This specification assumes that each group has its own baseline success rate and that the two groups are a priori independent. However, as Ding & Dasgupta (2016) caution, the independent binomial specification is a convenient practice rather than an implication of Fisher’s sharp null and the CRE design.

A third alternative uses independent binomial distributions with a common success rate across groups by setting $p_1 = p_0 = \theta$ with $\theta \sim \text{Beta}(\alpha_c, \beta_c)$. Marginalizing over θ , we have

$$\pi_{\text{CR}}(a, b; \alpha_c, \beta_c) = \binom{n_1}{a} \binom{n_0}{b} \frac{B(a + b + \alpha_c, n_1 + n_0 - (a + b) + \beta_c)}{B(\alpha_c, \beta_c)}. \quad (9)$$

When $(\alpha_c, \beta_c) = (1, 1)$, the induced distribution of the FRT p -value is close to the uniform distribution on $(0, 1)$ up to discreteness.

3.2.2 Monte Carlo Sampling and Aggregation

When both n_1 and n_0 are moderate, one can compute the posterior distribution for p_{FRT} by enumerating all $(a, b) \in \{0, \dots, n_1\} \times \{0, \dots, n_0\}$. This requires $O(n_1 n_0)$ operations to compute and normalize the weights $w(a, b)$. For each pair, evaluating the tail sum in (5) takes $O(\min\{n_1, n_0\})$ time, resulting in an overall complexity of $O(n_1 n_0 \times \min\{n_1, n_0\})$.

For large (n_1, n_0) , it can be preferable to sample from the posterior distribution $\gamma(a, b)$ rather than exhaustively evaluate the entire grid. A Metropolis-Hastings sampler for drawing

from $\gamma(a, b)$ is provided in the supplementary material. When the prior distribution can be factorized as $\pi(a, b) = \pi_1(a)\pi_0(b)$, as in the case of (7) and (8), $\gamma(a, b)$ factorizes as $\gamma(a, b) = \gamma_{11}(a)\gamma_{01}(b)$, where $\gamma_{11}(a) \propto \pi_1(a)\kappa_\rho(\tilde{n}_{11} - a)$ and $\gamma_{01}(b) \propto \pi_0(b)\kappa_\rho(\tilde{n}_{01} - b)$. As a result, we can sample $a^{(r)} \sim \gamma_{11}$ and $b^{(r)} \sim \gamma_{01}$ independently at each iteration $r = 1, \dots, R$ of the sampler. The cost of normalizing the two distributions is $O(n_1 + n_0)$; sampling R pairs is $O(R)$; and, evaluating the p -value for each draw via (5) costs $O(\min\{n_1, n_0\})$ per sample. The resulting total computational cost is $O(n_1 + n_0 + R \min\{n_1, n_0\})$.

Given Monte Carlo samples $\{(a^{(r)}, b^{(r)})\}_{r=1}^R$, posterior summaries are obtained by mapping each pair to $u^{(r)} = p_{a^{(r)}b^{(r)}}$ and aggregating over $\{u^{(r)}\}$. For example, the posterior mean can be approximated by $\tilde{p}_{\text{mean}} = \sum_{r=1}^R u^{(r)}/R$. The posterior distribution can be approximated by the empirical distribution of $\{u^{(r)}\}$, from which the posterior median and credible sets can be extracted. The MAP estimate can be obtained by tabulating the frequencies of the distinct values in $\{u^{(r)}\}$ and selecting the mode.

The Monte Carlo draws also enable posterior predictive generation of synthetic data and effect estimation. Specifically, each draw $(a^{(r)}, b^{(r)})$ determines $(n_{11}^{(r)}, n_{01}^{(r)}, n_{10}^{(r)}, n_{00}^{(r)}) = (a^{(r)}, b^{(r)}, n_1 - a^{(r)}, n_0 - b^{(r)})$. These counts can be released as multiply-imputed, synthetic data (Reiter 2003). Based on these tables, analysts also can compute estimands such as

$$\tau^{(r)} = \frac{a^{(r)}}{n_1} - \frac{b^{(r)}}{n_0}, \quad \text{RR}^{(r)} = \frac{a^{(r)}/n_1}{b^{(r)}/n_0}, \quad \text{OR}^{(r)} = \frac{a^{(r)}(n_0 - b^{(r)})}{(n_1 - a^{(r)})b^{(r)}}. \quad (10)$$

Here, $\tau^{(r)}$ is the risk difference, $\text{RR}^{(r)}$ is the risk ratio, and $\text{OR}^{(r)}$ is the odds ratio. Their empirical distributions provide point estimates and credible intervals of treatment effects.

4 Decision Making with DP-FRT-Bayes

After obtaining the privatized FRT p -value, one practice is to reject the null hypothesis when the p -value falls below a user-specified level α . However, under DP, the released

statistics include randomness introduced by the privacy mechanism. A principled decision rule should account for this uncertainty.

In this section, we base our decisions under DP-FRT-Bayes on $\Pr(p_{\text{FRT}} \leq \alpha \mid \tilde{\mathbf{n}})$, which represents the posterior probability that the FRT p -value does not exceed α . This quantity summarizes the strength of evidence for rejection, incorporates the full posterior shape rather than a single noisy point, and connects naturally to classical summaries such as posterior quantiles and one-sided credible bounds. We introduce two frameworks for implementing this decision-making process.

4.1 Bayes Risk-optimal Decision Framework

We first develop a Bayes rule that minimizes posterior risk of departing from the non-private decision. The aim is to recover as faithfully as possible the significance label that would be obtained without DP noise. Let the decision $\delta \in \{1, 0\}$ indicate reject and not reject, respectively. For fixed threshold $\alpha \in (0, 1)$, we consider the loss

$$L(\delta, p_{\text{FRT}}) = \begin{cases} \lambda_0, & \delta = 1, p_{\text{FRT}} > \alpha, \\ \lambda_1, & \delta = 0, p_{\text{FRT}} \leq \alpha, \\ 0, & (\delta = 0, p_{\text{FRT}} > \alpha) \text{ or } (\delta = 1, p_{\text{FRT}} \leq \alpha). \end{cases} \quad (11)$$

Here, $\lambda_0 > 0$ is the loss of being too aggressive, i.e., we reject in cases where the non-private test would not. Conversely, λ_1 is the loss of being too conservative, i.e., we fail to reject in cases where the non-private test would. The corresponding posterior risks given $\tilde{\mathbf{n}}$ are

$$R(\delta = 1 \mid \tilde{\mathbf{n}}) = \lambda_0 \Pr(p_{\text{FRT}} > \alpha \mid \tilde{\mathbf{n}}), \quad (12)$$

$$R(\delta = 0 \mid \tilde{\mathbf{n}}) = \lambda_1 \Pr(p_{\text{FRT}} \leq \alpha \mid \tilde{\mathbf{n}}). \quad (13)$$

The Bayes risk-optimal decision rule $\delta_{\text{Bayes}}(\tilde{\mathbf{n}}) = \arg \min_{\delta \in \{0,1\}} \mathbb{E}[L(\delta, p_{\text{FRT}}) \mid \tilde{\mathbf{n}}]$ is

$$\delta_{\text{Bayes}}(\tilde{\mathbf{n}}) = \begin{cases} 1, & R(\delta = 1 \mid \tilde{\mathbf{n}}) < R(\delta = 0 \mid \tilde{\mathbf{n}}) \iff \Pr(p_{\text{FRT}} \leq \alpha \mid \tilde{\mathbf{n}}) > \frac{\lambda_0}{\lambda_0 + \lambda_1} \\ 0, & \text{otherwise.} \end{cases} \quad (14)$$

This rule can be viewed as a decision based on a posterior quantile, where the quantile level is determined by the trade-off between the losses of being overly aggressive and overly conservative relative to the non-private decision. When there is no justification for assigning different losses to the two types of discordance, i.e., $\lambda_0 = \lambda_1$, the decision rule reduces to one based on the posterior median. The release of $\delta_{\text{Bayes}}(\tilde{\mathbf{n}})$ should be accompanied by $\Pr(p_{\text{FRT}} \leq \alpha \mid \tilde{\mathbf{n}})$, which conveys the strength of evidence supporting the decision.

4.1.1 Decision Confidence and Abstention under Uncertainty

When $\Pr(p_{\text{FRT}} \leq \alpha \mid \tilde{\mathbf{n}})$ is close to 1 or 0, there is strong evidence to reject or not, respectively. However, with a tight privacy budget or small sample size, the posterior for p_{FRT} can be diffuse due to the added noise, and this probability may lie near the binary Bayes threshold $\lambda_0/(\lambda_0 + \lambda_1)$. In such cases, the decision rule might be unreliable.

In the spirit of Chow's rule (Chow 1957, 1970), we equip the decision procedure with an explicit abstention option to deal with these situations. Specifically, we now let $\delta \in \{0, 1, u\}$, with u representing abstention, and $\lambda_u > 0$ be the loss incurred for abstaining, such as the operational cost of deferring the decision. The Bayes-optimal decision rule becomes

$$\delta_{\text{Bayes}}^*(\tilde{\mathbf{n}}) = \begin{cases} 1, & \Pr(p_{\text{FRT}} \leq \alpha \mid \tilde{\mathbf{n}}) > \max \left\{ \frac{\lambda_0}{\lambda_0 + \lambda_1}, 1 - \frac{\lambda_u}{\lambda_0} \right\}, \\ 0, & \Pr(p_{\text{FRT}} \leq \alpha \mid \tilde{\mathbf{n}}) < \min \left\{ \frac{\lambda_0}{\lambda_0 + \lambda_1}, \frac{\lambda_u}{\lambda_1} \right\}, \\ u, & \text{otherwise.} \end{cases} \quad (15)$$

As evident in (15) and illustrated in Figure 2, λ_u determines the width of the abstention region. Increasing λ_u reduces the width, thereby decreasing the likelihood of abstention.

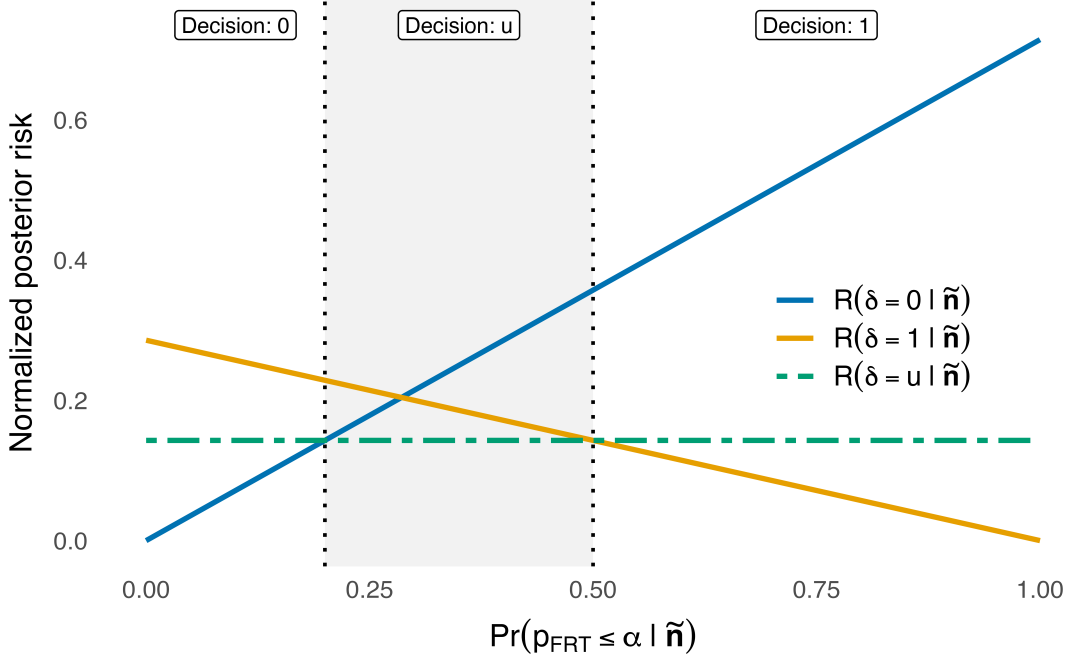


Figure 2: Illustration of the Bayes risk-optimal decision with an abstention option. The losses are specified as $\lambda_0 = 0.2$, $\lambda_1 = 0.5$, and $\lambda_u = 0.1$. The blue, orange, and green lines correspond to the posterior risks normalized by $(\lambda_0 + \lambda_1)$ for decisions $\delta = 0$, $\delta = 1$, and $\delta = u$, respectively. The shaded gray band marks the abstention region.

When λ_u is large relative to λ_0 and λ_1 , the abstention region degenerates, and (15) reduces to (14). Lemma 4.1 provides a sufficient and necessary condition.

Lemma 4.1. *The abstention option degenerates if and only if $\lambda_u \geq H/2$, where $H = (2\lambda_0\lambda_1)/(\lambda_0 + \lambda_1)$ is the harmonic mean of λ_0 and λ_1 .*

4.1.2 Sequential Decision under Additional Privacy Budget

Given an initial $\tilde{\mathbf{n}} = (\tilde{n}_{11}, \tilde{n}_{01})$, analysts who reach $\delta_{\text{Bayes}}^* = u$ may wish to improve decision certainty while still ensuring DP. In this section, we describe a sequential procedure to refine initial decisions. The basic idea is to augment the privacy budget and obtain additional noisy counts, which are used to update the posterior distributions and hence the decision.

Let $\epsilon_{\text{plus}} > 0$ be the added budget. We generate an independent, second noisy release

$$\tilde{\mathbf{n}}^+ = (\tilde{n}_{11}^+, \tilde{n}_{01}^+) = (n_{11} + \eta_{11}^+, n_{01} + \eta_{01}^+), \quad \eta_{11}^+, \eta_{01}^+ \stackrel{\text{i.i.d.}}{\sim} \text{Geom}(\exp(-\epsilon_{\text{plus}})). \quad (16)$$

The total privacy budget of the two releases is $\epsilon_{\text{tot}} = \epsilon + \epsilon_{\text{plus}}$ by the sequential composition property. Given $(\tilde{\mathbf{n}}^+, \tilde{\mathbf{n}})$, the posterior distribution becomes

$$\Pr(m_{11}, m_{01} \mid \tilde{\mathbf{n}}, \tilde{\mathbf{n}}^+) \propto \Pr(\tilde{\mathbf{n}}^+ \mid m_{11}, m_{01}) \Pr(\tilde{\mathbf{n}} \mid m_{11}, m_{01}) \pi(m_{11}, m_{01}). \quad (17)$$

Let $\gamma^+(a, b) = \Pr(m_{11} = a, m_{01} = b \mid \tilde{\mathbf{n}}, \tilde{\mathbf{n}}^+)$. Let $\rho_+ = \exp(-\epsilon_{\text{plus}}/\Delta f)$. By substituting the kernels from the Geometric mechanism defined in Section 2.2 with $\Delta f = 1$, we have

$$\gamma^+(a, b) = \frac{\pi(a, b) \kappa_\rho(\tilde{n}_{11} - a) \kappa_\rho(\tilde{n}_{01} - b) \kappa_{\rho_+}(\tilde{n}_{11}^+ - a) \kappa_{\rho_+}(\tilde{n}_{01}^+ - b)}{\sum_{a'=0}^{n_1} \sum_{b'=0}^{n_0} \pi(a', b') \kappa_\rho(\tilde{n}_{11} - a') \kappa_\rho(\tilde{n}_{01} - b') \kappa_{\rho_+}(\tilde{n}_{11}^+ - a') \kappa_{\rho_+}(\tilde{n}_{01}^+ - b')} \quad (18)$$

for $(a, b) \in \{0, \dots, n_1\} \times \{0, \dots, n_0\}$.

We now investigate how allocating additional privacy budget can improve decision certainty.

Denote the abstention region as

$$A = (t_{\text{low}}, t_{\text{high}}) = \left(\min \left\{ \frac{\lambda_0}{\lambda_0 + \lambda_1}, \frac{\lambda_u}{\lambda_1} \right\}, \max \left\{ \frac{\lambda_0}{\lambda_0 + \lambda_1}, 1 - \frac{\lambda_u}{\lambda_0} \right\} \right),$$

which is determined solely by the loss parameters. By allocating extra privacy budget, the posterior evidence of rejection given α is updated from $\Pr(p_{\text{FRT}} \leq \alpha \mid \tilde{\mathbf{n}})$ to $\Pr(p_{\text{FRT}} \leq \alpha \mid \tilde{\mathbf{n}}, \tilde{\mathbf{n}}^+)$, which may become more concentrated around 0 or 1. Hence, although the width of the abstention region remains fixed, the probability that the updated evidence falls within this abstention region may decrease. In fact, the chance of remaining in the abstention region decays exponentially in ϵ_{plus} , as shown in the supplementary material.

We can find an upper bound on how likely the refined posterior is to exit the abstention region after the top-up release. To do so, we adopt an information-theoretic perspective: conditioned on $\tilde{\mathbf{n}}$, the second release induces a channel whose ability to alter the posterior is governed by its total variation contraction under DP. By bounding this contraction and

relating posterior movement to the distance from the abstention boundaries, we obtain a sharp upper bound on the reduction of abstention probability.

To formalize this argument, let $\Psi = \Pr(p_{\text{FRT}} \leq \alpha \mid \tilde{\mathbf{n}})$ and $\Psi^+ = \Pr(p_{\text{FRT}} \leq \alpha \mid \tilde{\mathbf{n}}, \tilde{\mathbf{n}}^+)$. Let $S = \{0, \dots, n_1\} \times \{0, \dots, n_0\}$ denote the support of (m_{11}, m_{01}) . For $h \in \{0, 1\}$, let $S_h = \{(a, b) \in S : \mathbf{1}(p_{ab} \leq \alpha) = h\}$ be the subsets of S corresponding to acceptance ($h = 0$) and rejection ($h = 1$). Define the data-adaptive separation between these two classes by

$$\Delta(\tilde{\mathbf{n}}; \epsilon_{\text{plus}}) = \sum_{(a,b) \in S_1} \sum_{(a',b') \in S_0} \mu_1(a,b) \mu_0(a',b') s(\epsilon_{\text{plus}} (|a - a'| + |b - b'|)),$$

where $\mu_h(a, b) = \Pr(n_{11} = a, n_{01} = b \mid H = h, \tilde{\mathbf{n}})$ and $s(x) = \tanh(x/2)$. This quantity can be computed without accessing any private data. Theorem 4.2 presents the upper bound.

Theorem 4.2. *Let $A = (t_{\text{low}}, t_{\text{high}})$ be the abstention region with $0 < t_{\text{low}} < t_{\text{high}} < 1$, and define $r(\Psi) = \min\{\Psi - t_{\text{low}}, t_{\text{high}} - \Psi\}$ whenever $\Psi \in A$. Then, for every $\epsilon_{\text{plus}} > 0$,*

$$\Pr(\Psi^+ \notin A \mid \Psi \in A) \leq 2 \mathbb{E} \left(\frac{\Psi(1 - \Psi)}{r(\Psi)} \Delta(\tilde{\mathbf{n}}; \epsilon_{\text{plus}}) \mid \Psi \in A \right). \quad (19)$$

The quantity $s(\epsilon)$ is the standard conversion from a privacy budget ϵ to an upper bound on the adversary's distinguishing advantage between neighboring datasets, measured by the total variation distance between their output distributions under an ϵ -DP mechanism (Ghazi & Issa 2024). Theorem 4.2 shows that, under the additional privacy budget ϵ_{plus} , the probability of exiting the abstention region is controlled by a data-adaptive weighted average of the total variation bounds $s(\cdot)$ over acceptance and rejection classes.

Corollary 4.3 quantifies a necessary lower bound on ϵ_{plus} for ensuring that the refined posterior escapes the abstention region with high probability.

Corollary 4.3. *Let $A = (t_{\text{low}}, t_{\text{high}})$ be the abstention region with $0 < t_{\text{low}} < t_{\text{high}} < 1$. Fix a confidence level $1 - \xi \in (0, 1)$. For $\Psi \in A$, if the refined posterior Ψ^+ satisfies*

$\Pr(\Psi^+ \notin A \mid \tilde{\mathbf{n}}) \geq 1 - \xi$, then

$$\epsilon_{\text{plus}} \geq \inf \left\{ \epsilon > 0 : \Delta(\tilde{\mathbf{n}}; \epsilon) \geq \frac{(1 - \xi) r(\Psi)}{2\Psi(1 - \Psi)} \right\}. \quad (20)$$

where $r(\Psi) = \min\{\Psi - t_{\text{low}}, t_{\text{high}} - \Psi\}$, and $\Delta(\tilde{\mathbf{n}}; \epsilon)$ is defined as in Theorem 4.2.

The necessary ϵ_{plus} depends on ξ , Ψ , and Δ . Together, these quantities capture (i) how different the acceptance and rejection classes are under the current release (through Δ), (ii) how confident a decision the analyst requires (through ξ), and (iii) how close the current posterior is to the abstention boundary (through $r(\Psi)$). When the acceptance and rejection configurations are less distinguishable under the top-up mechanism (smaller Δ at a given ϵ_{plus}), when higher confidence is required (smaller ξ), or when the current posterior lies deeper inside the abstention region (larger $r(\Psi)$), a larger additional privacy budget is needed to push the decision outside the abstention region. A detailed algorithm for calculating the lower bound in (20) is presented in the supplementary material.

In practice, when the decision rule in (15) abstains, the analyst can select ϵ_{plus} larger than the lower bound in (20) for a pre-specified confidence level, e.g., $\xi = 0.05$ for 95% certainty. If the decision still abstains after generating $\tilde{\mathbf{n}}^+$, the analyst can repeat the procedure (if it is acceptable to increase the total privacy budget), or terminate and report the decision as inconclusive. This strategy spends privacy budget adaptively and only when necessary, allowing practitioners to decide at each stage whether to continue.

4.2 Frequentist-calibrated Decision Framework

We next calibrate a threshold to control frequentist type I error based on the posterior quantity $\Pr(p_{\text{FRT}} \leq \alpha \mid \tilde{\mathbf{n}})$. Specifically, define

$$\delta_{\text{Freq}} = \begin{cases} 1, & \Pr(p_{\text{FRT}} \leq \alpha \mid \tilde{\mathbf{n}}) > t^*, \\ 0, & \text{otherwise,} \end{cases} \quad (21)$$

where the threshold $t^* \in [0, 1]$ is chosen as the smallest value such that, under H_0^F , $\Pr(\delta_{\text{Freq}} = 1) \leq \alpha_{\text{Freq}}$, using α_{Freq} to denote the target type I error level. Specifically, let F_Ψ be the distribution of $\Pr(p_{\text{FRT}} \leq \alpha \mid \tilde{\mathbf{n}})$ under H_0^F . Its $(1 - \alpha_{\text{Freq}})$ -quantile,

$$t^* = F_\Psi^{-1}(1 - \alpha_{\text{Freq}}) = \inf\{t \in [0, 1] : F_\Psi(t) > 1 - \alpha_{\text{Freq}}\}, \quad (22)$$

yields the desired calibrated threshold. Equivalently, (21) can be viewed as a FRT based on the test statistic $\Psi = \Pr(p_{\text{FRT}} \leq \alpha \mid \tilde{\mathbf{n}})$, which rejects the null if its FRT p -value is at or below the target level α_{Freq} .

To determine the critical value t^* defined in (22), the key step is to derive F_Ψ , the distribution of Ψ under the sharp null hypothesis. However, the construction of F_Ψ depends on the total number of successes, $n_{+1} = n_{11} + n_{01}$, which is also subject to privatization and therefore unknown. Two calibration strategies are proposed below.

4.2.1 Worst-case Calibration

We first construct a threshold that is valid for all possible total numbers of successes. For each $K \in \{0, \dots, n\}$, let Q_K denote the probability mass function of $\tilde{\mathbf{n}} = (\tilde{n}_{11}, \tilde{n}_{01})$ under H_0^F with total number of successes equal to K , given by

$$Q_K(a, b) = \sum_{t=\max\{0, K-n_0\}}^{\min\{n_1, K\}} \frac{\binom{K}{t} \binom{n-K}{n_1-t}}{\binom{n}{n_1}} \kappa_\rho(a-t) \kappa_\rho(b-(K-t)) \quad (23)$$

for $(a, b) \in \{0, \dots, n_1\} \times \{0, \dots, n_0\}$. We define $F_\Psi^{(K)}$ as the cumulative distribution function of $\Psi = \Pr(p_{\text{FRT}} \leq \alpha \mid \tilde{\mathbf{n}})$ when $\tilde{\mathbf{n}} \sim Q_K$, that is,

$$F_\Psi^{(K)}(t) = \sum_{a=0}^{n_1} \sum_{b=0}^{n_0} Q_K(a, b) \mathbf{1}(\Psi \leq t), \quad t \in [0, 1], \quad (24)$$

and denote $t_K = \inf\{t : F_\Psi^{(K)}(t) > 1 - \alpha_{\text{Freq}}\}$ as the right-continuous $(1 - \alpha_{\text{Freq}})$ -quantile of $F_\Psi^{(K)}$. We set the threshold as $t_{\text{LFC}}^* = \sup_{K \in \{0, \dots, n\}} t_K$. This leads to the decision rule

$$\delta_{\text{LFC}}(\tilde{\mathbf{n}}) = \begin{cases} 1, & \Pr(p_{\text{FRT}} \leq \alpha \mid \tilde{\mathbf{n}}) > t_{\text{LFC}}^*, \\ 0, & \text{otherwise.} \end{cases} \quad (25)$$

Theorem 4.4 ensures type I error control under (25).

Theorem 4.4. *Under the sharp null H_0^F , we have $\Pr(\delta_{\text{LFC}}(\tilde{\mathbf{n}}) = 1) \leq \alpha_{\text{Freq}}$, where the probability averages over randomization and the privacy mechanism.*

In practice, the threshold can be approximated by simulation. For any value of $K \in \{0, \dots, n\}$, we take a random draw of the number of successes in the treated group, $a_{11} \sim \text{Hypergeometric}(n, K, n_1)$, and set $b_{01} = K - a_{11}$. We apply the Geometric mechanism to (a_{11}, b_{01}) to generate $(\tilde{a}_{11}, \tilde{b}_{01})$. Using these simulated noisy counts, we compute $\Pr(p_{\text{FRT}} \leq \alpha \mid \tilde{a}_{11}, \tilde{b}_{01})$. We repeat this process many times and approximate $F_{\Psi}^{(K)}$ using its empirical distribution. We estimate t_K using the right-continuous empirical quantile of this simulated distribution. We perform this simulation for each $K = 0, \dots, n$ and set $t_{\text{LFC}}^* = \sup_K t_K$. A detailed algorithm is presented in the supplementary material.

4.2.2 Data-adaptive Calibration with Confidence Sets

Instead of the worst case, we can use a data-adaptive confidence set for n_{+1} . For each K , order the lattice points $(a, b) \in \{0, \dots, n_1\} \times \{0, \dots, n_0\}$ by decreasing $Q_K(a, b)$. We take the smallest set A_K whose total mass is at least $1 - \zeta$, with $\zeta \in (0, \alpha_{\text{Freq}})$. Define the $(1 - \zeta)$ -confidence set, $C_{1-\zeta}(\tilde{\mathbf{n}}) = \{K \in \{0, \dots, n\} : \tilde{\mathbf{n}} \in A_K\}$. For $\alpha' = \alpha_{\text{Freq}} - \zeta$, define $t'_K = \inf\{t : F_{\Psi}^{(K)}(t) > 1 - \alpha'\}$ as the right-continuous $(1 - \alpha')$ quantile of $F_{\Psi}^{(K)}$ from (24). Letting $t_{\text{Neyman}}^* = \sup_{K \in C_{1-\zeta}(\tilde{\mathbf{n}})} t'_K$, the decision rule is

$$\delta_{\text{Neyman}}(\tilde{\mathbf{n}}) = \begin{cases} 1, & \Pr(p_{\text{FRT}} \leq \alpha \mid \tilde{\mathbf{n}}) > t_{\text{Neyman}}^*, \\ 0, & \text{otherwise.} \end{cases} \quad (26)$$

Intuitively, (26) spends at most ζ on coverage of n_{+1} and uses the least favorable threshold within the confidence set, which yields type I error control while typically reducing conservativeness. One can choose $\zeta = 0.05$ to make $C_{1-\zeta}(\tilde{\mathbf{n}})$ a 95% confidence set. Lemma 4.5 and Theorem 4.6 formally state the frequentist properties of the data-adaptive procedure.

Lemma 4.5. For each K , we have $\Pr_K(K \in C_{1-\zeta}(\tilde{\mathbf{n}})) = \Pr_K(\tilde{\mathbf{n}} \in A_K) \geq 1 - \zeta$, where \Pr_K denotes probability under Q_K .

Theorem 4.6. Fix $\zeta \in (0, \alpha_{\text{Freq}})$ and set $\alpha' = \alpha_{\text{Freq}} - \zeta$. Under the sharp null H_0^{F} , we have $\Pr(\delta_{\text{Neyman}}(\tilde{\mathbf{n}}) = 1) \leq \alpha_{\text{Freq}}$.

We can approximate t_{Neyman}^* using simulation, proceeding as in the simulation in Section 4.2.1. However, after obtaining $(\tilde{a}_{11}, \tilde{b}_{01})$, we use their empirical distribution to approximate Q_K . We construct A_K as the smallest empirical set with probability mass at least $1 - \zeta$. We form the set $C_{1-\zeta}(\tilde{\mathbf{n}})$, estimate $F_{\Psi}^{(K)}$, compute t'_K , and finally set t_{Neyman}^* to determine the decision rule. A detailed algorithm is presented in the supplementary material.

5 Simulation Studies and Data Analysis

This section presents simulation studies that illustrate the performance of DP-FRT-Bayes. We also apply DP-FRT-Bayes to the ADAPTABLE trial data (Jones et al. 2021). Code for reproducing the results is available at https://github.com/qy-sun/dp_frt.

5.1 Assessing DP-FRT-Bayes Estimates of p -value

We first evaluate the ability of DP-FRT-Bayes to estimate the FRT p -value. To do so, we fix four sets of $(n_{11}, n_{10}, n_{01}, n_{00})$ at the values displayed in Table 1. For each dataset, we generate 1000 independent draws of privatized $\tilde{\mathbf{n}}$ and estimate the posterior distribution of p_{FRT} using the methods from Section 3.2.

Table 2 reports the simulated biases of the posterior mean \tilde{p}_{mean} , as well as the percentages of the 1000 intervals based on the 95% credible sets that cover the non-private p_{FRT} and the average width of those intervals. The posterior means offer reasonable estimates of p_{FRT} , particularly when $n \geq 500$ and $\epsilon \geq 0.5$. When $\epsilon = 0.2$, the posterior mean tends to be

Table 1: Settings for the simulation studies in Section 5.1 of how accurately DP-FRT-Bayes estimates the non-private p -value, p_{FRT} .

Case	n_{11}	n_{10}	n_{01}	n_{00}	p_{FRT}
Case 1: No effect	25	25	25	25	0.579
	125	125	125	125	0.536
	250	250	250	250	0.525
Case 2: Small effect	28	22	25	25	0.344
	138	112	125	125	0.141
	275	225	250	250	6.43×10^{-2}
Case 3: Medium effect	30	20	25	25	0.211
	150	100	125	125	1.54×10^{-2}
	300	200	250	250	9.14×10^{-4}
Case 4: Large effect	32	18	25	25	0.113
	162	88	125	125	5.54×10^{-4}
	325	175	250	250	1.05×10^{-6}

inaccurate unless $n = 1000$. The coverage of the intervals is slightly below 95% when $\epsilon = 0.2$ and near 95% when $\epsilon \geq 0.5$. When $n = 100$, the intervals tend to be wide, suggesting that DP-FRT-Bayes at this small sample size is not particularly informative. Indeed, when $\epsilon = 0.2$ and $n = 100$, the intervals typically cover nearly the full support of p_{FRT} . This is not surprising, as the noise from DP often can swamp signals when ϵ and n are small. When $n = 1000$, the interval widths decline, so that even with this modest sample size DP-FRT-Bayes offers reasonably precise inferences. We note that across all n , the interval widths are largest for the no effect scenarios. In these situations, the noisy counts can be

Table 2: Simulated biases of the posterior means, along with the coverage (%) and average width of the 95% credible sets in Cases 1–4 when $\epsilon \in \{0.2, 0.5, 1\}$.

Case	$\epsilon = 0.2$			$\epsilon = 0.5$			$\epsilon = 1$		
	Bias	Cov	Width	Bias	Cov	Width	Bias	Cov	Width
(a) $n = 100$									
1: No effect	-0.059	93.5	0.938	-0.022	95.0	0.797	-0.007	95.0	0.538
2: Small	0.093	94.2	0.935	0.033	94.8	0.780	0.025	95.6	0.520
3: Medium	0.174	94.2	0.920	0.089	96.0	0.721	0.024	95.1	0.431
4: Large	0.211	94.8	0.902	0.095	95.1	0.621	0.030	96.1	0.324
(b) $n = 500$									
1: No effect	-0.024	93.6	0.835	-0.005	94.0	0.500	0.002	95.1	0.275
2: Small	0.099	94.3	0.704	0.027	93.7	0.323	0.008	95.6	0.162
3: Medium	0.077	93.4	0.406	0.012	94.9	0.085	0.002	95.3	0.032
4: Large	0.020	94.1	0.132	0.001	94.0	0.009	0.000	95.7	0.002
(c) $n = 1000$									
1: No effect	-0.004	92.8	0.732	0.003	93.6	0.376	-0.001	96.1	0.198
2: Small	0.066	93.6	0.419	0.011	96.1	0.137	0.003	96.7	0.065
3: Medium	0.009	93.4	0.058	0.001	95.0	0.006	0.000	96.5	0.002
4: Large	0.000	91.5	0.003	0.000	94.7	0.000	0.000	94.3	0.000

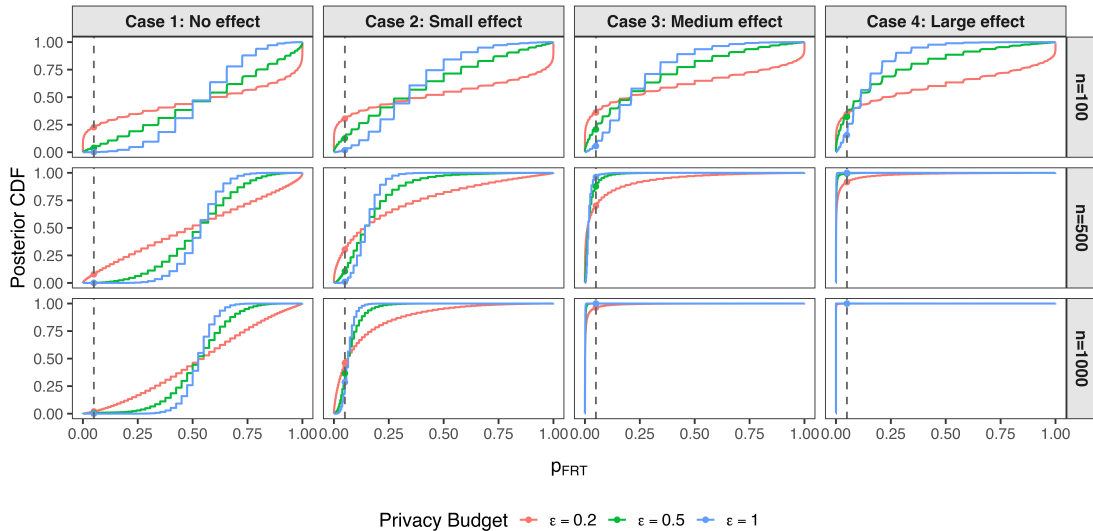


Figure 3: Posterior CDF for DP-FRT-Bayes p -value from 100 runs in Cases 1–4 when $\epsilon \in \{0.2, 0.5, 1\}$. Vertical black dashed line indicates the nominal significance level $\alpha = 0.05$.

consistent with a relatively wide range of plausible true counts, which in turn correspond to a relatively wide range of plausible p -values.

As a further illustration of the behavior of DP-FRT-Bayes, Figure 3 displays the cumulative distribution function (CDF) of all posterior draws of the DP-FRT-Bayes p -value from 100 runs of each scenario. The CDF shifts upward when the treatment effect size increases, leading to higher values of Ψ and stronger evidence against the null.

The supplementary material includes additional simulation results. They show that the posterior mean and median perform similarly and are slightly preferable to the MAP as a point estimator of p_{FRT} . They also show that results are similar under the independent Beta-binomial prior of (8) and the common success rate Beta prior of (9).

5.2 Evaluating Decision Rules under DP-FRT-Bayes

We next consider the decision rules described in Section 4. We fix twelve sets of potential outcomes $\{Y_i(1), Y_i(0)\}_{i=1}^n$ representing different study populations and treatment effects,

Table 3: Simulation settings for repeated sampling studies of causal inferences in Section 5.2. $N_{11} = \sum_{i=1}^n Y_i(1)$, $N_{10} = \sum_{i=1}^n 1 - Y_i(1)$, $N_{01} = \sum_{i=1}^n Y_i(0)$, $N_{00} = \sum_{i=1}^n 1 - Y_i(0)$.

Case	N_{11}	N_{10}	N_{01}	N_{00}
	50	50	50	50
Case 5: No effect ($\tau = 0$)	250	250	250	250
	500	500	500	500
	55	45	50	50
Case 6: Small effect ($\tau = 0.05$)	275	225	250	250
	550	450	500	500
	60	40	50	50
Case 7: Medium effect ($\tau = 0.1$)	300	200	250	250
	600	400	500	500
	65	35	50	50
Case 8: Large effect ($\tau = 0.15$)	325	175	250	250
	650	350	500	500

summarized in Table 3. In each study population, we randomly assign n_1 out of n units to the treatment group. This results in a realized outcome table, $(n_{11}, n_{10}, n_{01}, n_{00})$. We then apply DP-FRT-Bayes. We compute the Bayes-optimal decision using loss parameters $(\lambda_0, \lambda_1, \lambda_u) = (1, 1, 0.025)$ with the nominal significance level at $\alpha = 0.05$. We repeat this process 1000 times for each scenario. Analogous results for the frequentist decision rule are in the supplementary material. The supplementary material includes simulations illustrating the use of DP-FRT-Bayes for sequential decision-making as in Section 4.1.2.

Figure 4 summarizes the relative frequencies of each decision in the Bayes risk-optimal rule

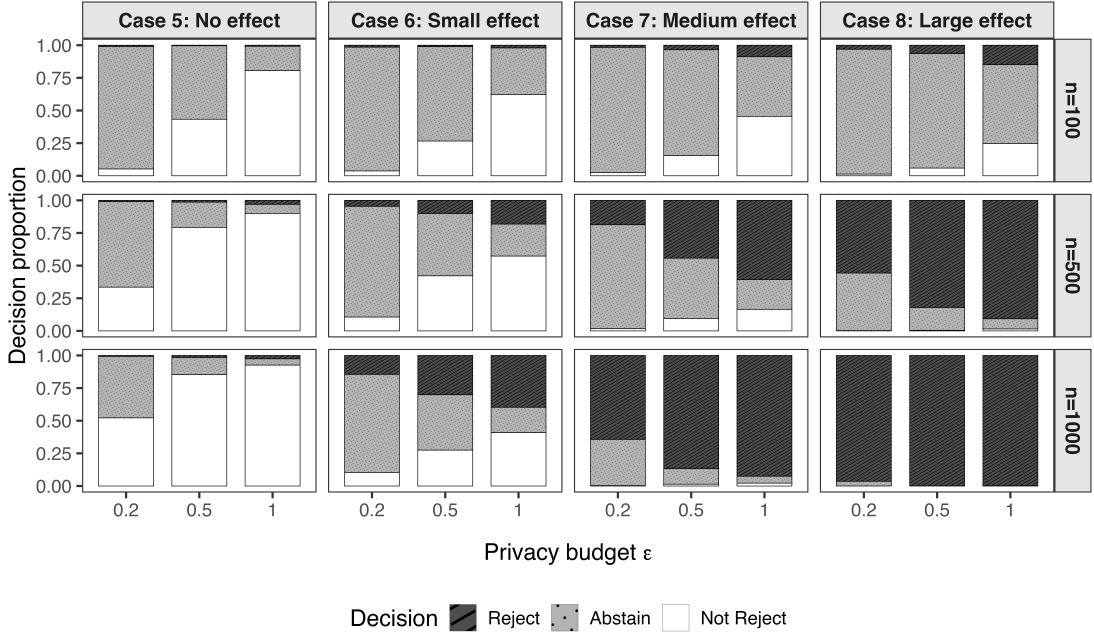


Figure 4: Decisions of the Bayes risk-optimal rule with abstention for $\epsilon \in \{0.2, 0.5, 1\}$ in Cases 5–8 for $n \in \{100, 500, 1000\}$ with $(\lambda_0, \lambda_1, \lambda_u) = (1, 1, 0.025)$.

with abstention under the different study populations when $\epsilon \in \{0.2, 0.5, 1\}$. When $\epsilon = 0.2$, the proportion of abstentions can be substantial, particularly when $n = 100$, reflecting greater decision uncertainty induced by the relatively large impacts of adding DP noise. As ϵ or n increase, abstentions gradually diminish, and the proportions of correct rejections rise. For large effects, nearly all decisions favor rejection when either ϵ or n is sufficiently large, indicating that the Bayes risk-optimal rule can have power to detect treatment effects while managing privacy-induced uncertainty through the abstention option.

Figure 5 shows the rejection rates of the Bayes risk-optimal rule with abstention under varying loss parameters $(\lambda_0, \lambda_1, \lambda_u)$ across privacy budgets and sample sizes. The results highlight the sensitivity of decision outcomes to the relative weighting of rejection, non-rejection, and abstention losses. When λ_u is small, the rule tends to abstain more and reject less frequently, leading to lower rejection rates across all settings. As λ_u increases, abstention becomes less likely. Under the sharp null (Case 5), rejection rates remain near

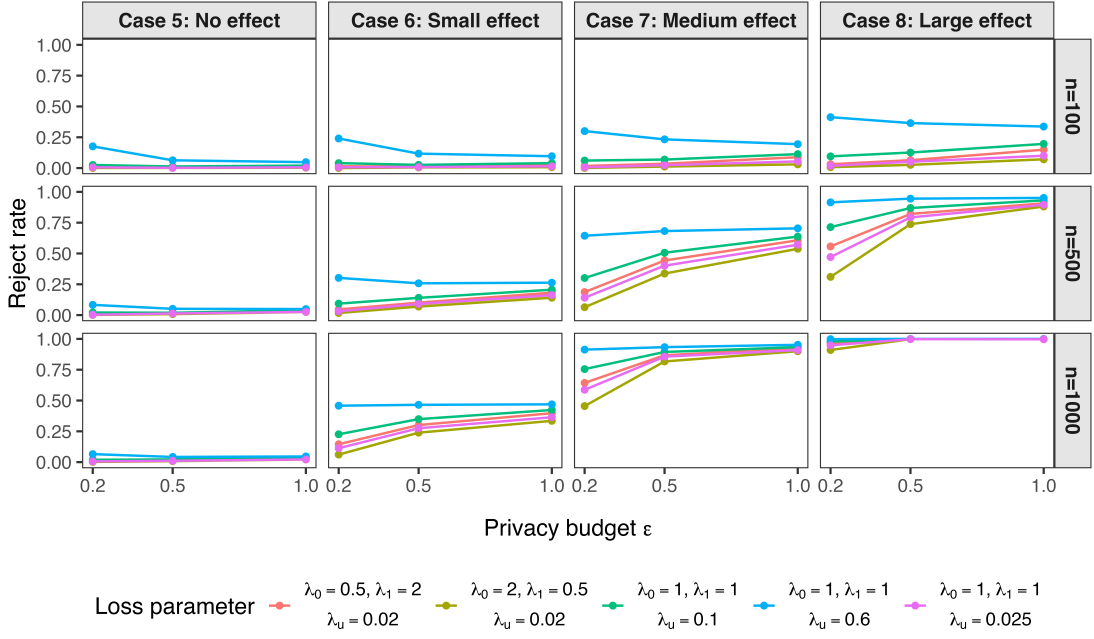


Figure 5: Rejection rates of the Bayes risk-optimal rule with abstention under varying loss parameters $(\lambda_0, \lambda_1, \lambda_u)$ for $\epsilon \in \{0.2, 0.5, 1\}$ in Cases 5–8 under $n \in \{100, 500, 1000\}$.

zero across all loss parameters. For cases with genuine effects (Cases 6–8), rejection rates increase with both ϵ and n as expected.

5.3 Analysis of ADAPTABLE trial

In this section, we illustrate the DP-FRT-Bayes framework using data from the ADAPTABLE trial (Jones et al. 2021). This is a randomized comparison of two daily aspirin dosing strategies for secondary prevention in patients with established atherosclerotic cardiovascular disease. We analyze the data under intention-to-treat assignment of taking 81 mg ($Z = 0; n_0 = 7540$) versus 325 mg ($Z = 1; n_1 = 7536$) aspirin. The binary outcome Y is a composite of death from any cause, hospitalization for myocardial infarction, or hospitalization for stroke. At median followup, we have $(n_{11}, n_{10}, n_{01}, n_{00}) = (569, 6967, 590, 6950)$. The non-private FRT p -value is 0.746, offering essentially no evidence against the sharp null hypothesis of no difference between the 325 mg and 81 mg aspirin groups.

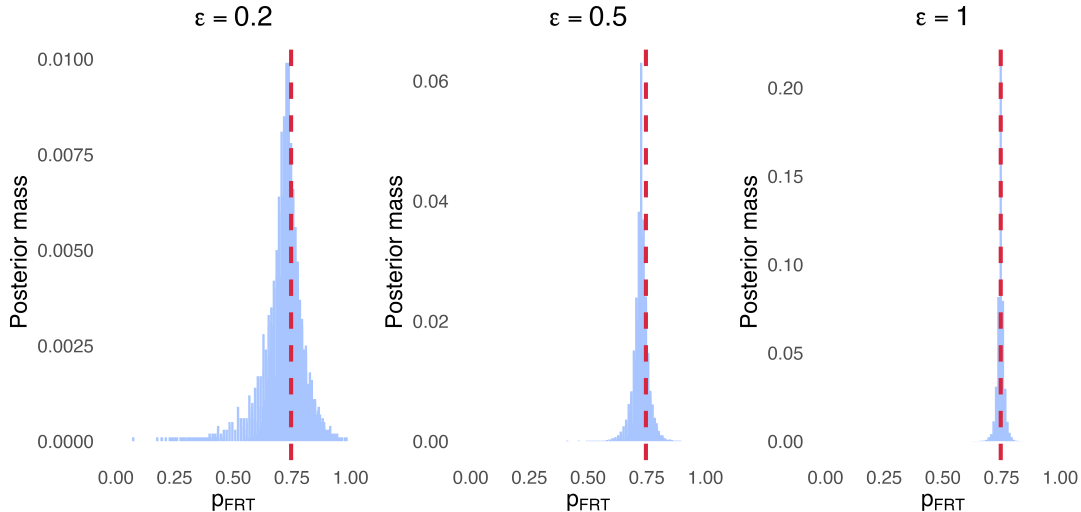


Figure 6: Posterior distributions of DP-FRT-Bayes p -value under $\epsilon \in \{0.2, 0.5, 1\}$ in the ADAPTABLE trial. Red dashed lines indicate the non-private p -value of 0.746.

For illustrative purposes, we apply DP-FRT-Bayes using $\epsilon \in \{0.2, 0.5, 1\}$, where $\alpha = 0.05$ and loss parameters $\lambda_0 = \lambda_1 = 1$ and $\lambda_u = 0.025$. As shown in Figure 6, the posterior distributions of the differentially private FRT p -values increasingly concentrate around the non-private counterpart as the privacy budget grows, with most of the posterior mass remaining well away from the rejection region. The posterior rejection probabilities Ψ are nearly zero across all privacy levels, yielding a Bayes-optimal decision of “do not reject.”

6 Discussion

We develop a framework for differentially private FRTs for binary outcomes, including methods for differentially private estimation of the FRT p -value and formal decision rules for hypothesis testing. The methods exhibit reasonable finite-sample performance while also supporting uncertainty quantification and adaptive use of privacy budgets.

The DP-FRT methods can be extended directly to bounded discrete responses, such as ordinal or count data with finite support. For bounded continuous responses, direct

application of the binary FRT requires discretization or binning. A principled approach is to treat the binning as a latent process and marginalize over the latent contingency tables rather than conditioning on a fixed discretization. This can be embedded within the Bayesian denoising framework, thereby propagating both binning and DP-induced uncertainties.

The DP-FRT methods can be generalized beyond CREs to stratified or block-randomized designs, paired or cluster randomization, and rerandomization procedures. In each case, the structure of the assignment mechanism changes the randomization distribution but does not affect the privacy mechanism applied to the observed outcomes. Combining DP-FRT with covariate-adjusted or rerandomized FRTs may improve efficiency, though the resulting randomization distributions will generally depend on more complex sufficient statistics requiring tailored privacy analysis.

Another promising direction is to extend the DP-FRT framework to the testing of weak null hypotheses (Ding & Dasgupta 2018, Wu & Ding 2021). Under weak nulls, exact randomization inference is generally infeasible without additional modeling or asymptotic justification, because unit-level treatment effects are not fully specified. A natural bridge arises through the posterior predictive checking framework (Rubin 1984, Meng 1994), where one computes posterior predictive p -values by averaging the FRT p -values over the posterior distribution of unobserved potential outcomes. Incorporating this averaging into the DP-FRT could yield a unified framework for privacy-preserving inference under both sharp and weak nulls.

Certain designs naturally induce non-sensitive randomization distributions. For example, under matched-pair randomization, the paired sign test depends only on the number of discordant pairs and not on individual outcomes. Consequently, the randomization distribution itself requires no privacy noise, which instead can be applied only to the

observed test statistic. Further exploration of design-adaptive privacy mechanisms could result in algorithms with increased accuracy for a given privacy cost.

Disclosure statement

On behalf of all authors, the corresponding author states that there is no conflict of interest.

Data Availability Statement

The data analyzed in this study are derived from the summary reported in the published ADAPTABLE trial (Jones et al. 2021). No individual-level or proprietary data were accessed. All quantities required to reproduce the analyses are fully contained within the manuscript; therefore, no additional data are publicly archived.

References

- Abowd, J. M., Ashmead, R., Cumings-Menon, R., Garfinkel, S., Heineck, M., Heiss, C. et al. (2022), ‘The 2020 Census Disclosure Avoidance System TopDown Algorithm’, *Harvard Data Science Review* .
- Awan, J. & Slavković, A. (2018), Differentially private uniformly most powerful tests for binomial data, *in* ‘Proceedings of the 32nd International Conference on Neural Information Processing Systems’, Curran Associates Inc., pp. 4212–4222.
- Chow, C. (1957), ‘An optimum character recognition system using decision functions’, *IRE Transactions on Electronic Computers* **EC–6**(4), 247–254.
- Chow, C. (1970), ‘On optimum recognition error and reject tradeoff’, *IEEE Transactions on Information Theory* **16**(1), 41–46.

- Couch, S., Kazan, Z., Shi, K., Bray, A. & Groce, A. (2019), Differentially private non-parametric hypothesis testing, *in* ‘Proceedings of the 2019 ACM SIGSAC Conference on Computer and Communications Security’, ACM, pp. 737–751.
- Ding, P. & Dasgupta, T. (2016), ‘A potential tale of two-by-two tables from completely randomized experiments’, *Journal of the American Statistical Association* **111**(513), 157–168.
- Ding, P. & Dasgupta, T. (2018), ‘A randomization-based perspective on analysis of variance: a test statistic robust to treatment effect heterogeneity’, *Biometrika* **105**(1), 45–56.
- Dinur, I. & Nissim, K. (2003), Revealing information while preserving privacy, *in* ‘Proceedings of the Twenty-second ACM SIGMOD-SIGACT-SIGART Symposium on Principles of Database Systems’, ACM, pp. 202–210.
- D’Orazio, V., Honaker, J. & King, G. (2015), ‘Differential privacy for social science inference’, Sloan Foundation Economics Research Paper No. 2676160. Available at SSRN: <https://ssrn.com/abstract=2676160>.
- Dwork, C. (2006), Differential privacy, *in* ‘International Colloquium on Automata, Languages, and Programming’, Vol. 4052, Springer, pp. 1–12.
- Dwork, C., McSherry, F., Nissim, K. & Smith, A. (2006), Calibrating noise to sensitivity in private data analysis, *in* ‘Theory of Cryptography Conference’, Vol. 3876, Springer, pp. 265–284.
- Dwork, C., Smith, A., Steinke, T. & Ullman, J. (2017), ‘Exposed! a survey of attacks on private data’, *Annual Review of Statistics and Its Application* **4**(1), 61–84.
- Fisher, R. A. (1935), *The Design of Experiments*, 1st edn, Oliver and Boyd, Edinburgh.
- Gaboardi, M., Lim, H., Rogers, R. & Vadhan, S. (2016), Differentially private chi-squared

- hypothesis testing: Goodness of fit and independence testing, *in* ‘International Conference on Machine Learning’, Vol. 48, PMLR, pp. 2111–2120.
- Ghazi, E. & Issa, I. (2024), ‘Total variation meets differential privacy’, *IEEE Journal on Selected Areas in Information Theory* **5**, 207–220.
- Ghosh, A., Roughgarden, T. & Sundararajan, M. (2012), ‘Universally utility-maximizing privacy mechanisms’, *SIAM Journal on Computing* **41**(6), 1673–1693.
- Guha, S. & Reiter, J. P. (2025), ‘Differentially private estimation of weighted average treatment effects for binary outcomes’, *Computational Statistics & Data Analysis* **207**, 108145.
- Jones, W. S., Mulder, H., Wruck, L. M., Pencina, M. J., Kripalani, S., Muñoz, D. et al. (2021), ‘Comparative effectiveness of aspirin dosing in cardiovascular disease’, *New England Journal of Medicine* **384**(21), 1981–1990.
- Kalemaj, I., Kasiviswanathan, S. & Ramdas, A. (2024), Differentially private conditional independence testing, *in* ‘International Conference on Artificial Intelligence and Statistics’, Vol. 238, PMLR, pp. 3700–3708.
- Kazan, Z. & Reiter, J. P. (2024a), ‘Bayesian inference under differential privacy with bounded data’, *arXiv preprint arXiv:2405.13801* .
- Kazan, Z. & Reiter, J. P. (2024b), Prior-itzing privacy: A Bayesian approach to setting the privacy budget in differential privacy, *in* A. Globerson, L. Mackey, D. Belgrave, A. Fan, U. Paquet, J. Tomczak & C. Zhang, eds, ‘Advances in Neural Information Processing Systems’, Vol. 37, Curran Associates, Inc., pp. 90384–90430.
- Kazan, Z., Shi, K., Groce, A. & Bray, A. P. (2023), The test of tests: A framework for differentially private hypothesis testing, *in* ‘International Conference on Machine Learning’, Vol. 202, PMLR, pp. 16131–16151.

- Lee, S. K., Gresele, L., Park, M. & Muandet, K. (2019), ‘Privacy-preserving causal inference via inverse probability weighting’, *arXiv preprint arXiv:1905.12592* .
- Meng, X. L. (1994), ‘Posterior predictive p -values’, *The Annals of Statistics* **22**(3), 1142–1160.
- Mukherjee, S., Mustafi, A., Slavković, A. & Vilhuber, L. (2024), Improving privacy for respondents in randomized controlled trials: A differential privacy approach, *in* R. Gong, V. J. Hotz & I. M. Schmutte, eds, ‘Data Privacy Protection and the Conduct of Applied Research: Methods, Approaches and their Consequences’, University of Chicago Press.
- Niu, F., Nori, H., Quistorff, B., Caruana, R., Ngwe, D. & Kannan, A. (2022), Differentially private estimation of heterogeneous causal effects, *in* ‘Conference on Causal Learning and Reasoning’, Vol. 177, PMLR, pp. 618–633.
- Peña, V. & Barrientos, A. F. (2025), ‘Differentially private hypothesis testing with the subsampled and aggregated randomized response mechanism’, *Statistica Sinica* **35**, 671–691.
- Reiter, J. P. (2003), ‘Inference for partially synthetic, public use microdata sets’, *Survey Methodology* **29**(2), 181–188.
- Rubin, D. B. (1974), ‘Estimating causal effects of treatments in randomized and nonrandomized studies’, *Journal of Educational Psychology* **66**(5), 688–701.
- Rubin, D. B. (1984), ‘Bayesianly justifiable and relevant frequency calculations for the applied statistician’, *The Annals of Statistics* **12**(4), 1151–1172.
- Wu, J. & Ding, P. (2021), ‘Randomization tests for weak null hypotheses in randomized experiments’, *Journal of the American Statistical Association* **116**(536), 1898–1913.

Supplemental Material for “Differentially Private Fisher Randomization Tests for Binary Outcomes”

This supplementary material contains additional algorithmic details, simulation and theoretical results, and proofs of lemmas and theorems in the main text. Section S.1 provides detailed algorithms. Section S.2 shows results of additional simulation studies referenced in the main text. Section S.3 presents proofs of two results, namely that clipping does not influence the posterior inferences of DP-FRT-Bayes and that the probability of escaping the abstention region when spending additional privacy budget decays exponentially. Section S.4 includes proofs and derivations of lemmas and theorems.

S.1 Algorithms and Implementation Details

S.1.1 MCMC Samplers for Posterior Computation

The following two algorithms provide implementation details for posterior computation in Section 3.2 of the main text. Algorithm S.1 describes a generic Metropolis-Hastings sampler and Algorithm S.2 illustrates a sampler tailored for the common success rate Beta prior.

Algorithm S.1: Metropolis-Hastings Sampler for $\gamma(a, b)$

Input: group sizes (n_1, n_0) ; privatized counts $\tilde{\mathbf{n}} = (\tilde{n}_{11}, \tilde{n}_{01})$; prior $\pi(a, b)$; privacy budget ϵ ; Monte Carlo size R ; Burn-in size B .

Output: posterior samples $\{(a^{(r)}, b^{(r)})\}_{r=B+1}^{B+R}$ and the corresponding $\{p^{(r)}\}_{r=B+1}^{B+R}$.

Initialize $(a^{(0)}, b^{(0)})$ on $\{0, \dots, n_1\} \times \{0, \dots, n_0\}$;

for $r = 0, \dots, B + R - 1$ **do**

Draw an independent proposal $(a^*, b^*) \sim \pi(\cdot)$ for $(a, b) \in \{0, \dots, n_1\} \times \{0, \dots, n_0\}$;

Compute $\alpha_{\text{MH}} = \min \left\{ 1, \frac{\kappa_\rho(\tilde{n}_{11} - a^*)\kappa_\rho(\tilde{n}_{01} - b^*)}{\kappa_\rho(\tilde{n}_{11} - a^{(r)})\kappa_\rho(\tilde{n}_{01} - b^{(r)})} \right\}$;

Draw $U \sim \text{Unif}(0, 1)$ and set $(a^{(r+1)}, b^{(r+1)}) \leftarrow \begin{cases} (a^*, b^*), & U \leq \alpha_{\text{MH}}, \\ (a^{(r)}, b^{(r)}), & \text{otherwise.} \end{cases}$

Compute $p^{(r+1)} = p_{a^{(r+1)}b^{(r+1)}}$ via (5)

end

Use $\{(a^{(r)}, b^{(r)})\}_{r=B+1}^{B+R}$ as draws from $\gamma(a, b)$ and record the corresponding $\{p^{(r)}\}_{r=B+1}^{B+R}$.

Algorithm S.2: Metropolis-Hastings sampler for $\gamma(a, b)$ with common-rate prior

Input: group sizes (n_1, n_0) ; privatized counts $\tilde{\mathbf{n}} = (\tilde{n}_{11}, \tilde{n}_{01})$; common success rate Beta prior $\pi_{\text{CR}}(a, b)$; privacy budget ϵ ; Monte Carlo size R ; Burn-in size B .

Output: samples $\{(a^{(r)}, b^{(r)})\}_{r=B+1}^{B+R}$ from $\gamma(a, b)$ and the corresponding $\{p^{(r)}\}_{r=B+1}^{B+R}$.

Define $q_A(a) \propto \kappa_\rho(\tilde{n}_{11} - a)$ for $a = 0, \dots, n_1$ and $q_B(b) \propto \kappa_\rho(\tilde{n}_{01} - b)$ for $b = 0, \dots, n_0$;

Initialize $(a^{(0)}, b^{(0)})$ on $\{0, \dots, n_1\} \times \{0, \dots, n_0\}$;

for $r = 0, \dots, B + R - 1$ **do**

Draw $a^* \sim q_A(\cdot)$ and $b^* \sim q_B(\cdot)$ independently;

Compute $\alpha_{\text{MH}} = \min \left\{ 1, \frac{\pi_{\text{CR}}(a^*, b^*)}{\pi_{\text{CR}}(a^{(r)}, b^{(r)})} \right\}$;

Draw $U \sim \text{Unif}(0, 1)$ and set $(a^{(r+1)}, b^{(r+1)}) \leftarrow \begin{cases} (a^*, b^*), & U \leq \alpha_{\text{MH}}, \\ (a^{(r)}, b^{(r)}), & \text{otherwise.} \end{cases}$

Compute $p^{(r+1)} = p_{a^{(r+1)}b^{(r+1)}}$ via (5);

end

Use $\{(a^{(r)}, b^{(r)})\}_{r=B+1}^{B+R}$ as draws from $\gamma(a, b)$ and record the corresponding $\{p^{(r)}\}_{r=B+1}^{B+R}$.

S.1.2 Algorithm for Lower Bounding Additional Privacy Budget

Algorithm S.3 approximates the data-adaptive lower bound on the additional privacy budget ϵ_{plus} derived in Section 4.1.2 of the main text. We describe a bisection to find the smallest ϵ such that $\widehat{\Delta}(\epsilon) \geq \tau$, but any bracketing root-finding procedure can be used instead.

Algorithm S.3: Data-adaptive Lower Bound on the Additional Privacy Budget ϵ_{plus}

Input: abstention region A ; confidence level $1 - \xi \in (0, 1)$; significance level α ;
approximation size L ; tolerance tol ; current posterior γ and evidence Ψ .

Output: data-adaptive necessary lower bound ϵ_{lb} .

Compute $r(\Psi) = \min\{\Psi - t_{\text{low}}, t_{\text{high}} - \Psi\}$ and set $\tau = (1 - \xi) r(\Psi) / (2\Psi(1 - \Psi))$;

Set $\mu_1(a, b \mid \tilde{\mathbf{n}}) \propto \gamma(a, b) \mathbf{1}\{p_{ab} \leq \alpha\}$ and $\mu_0(a, b \mid \tilde{\mathbf{n}}) \propto \gamma(a, b) \mathbf{1}\{p_{ab} > \alpha\}$;

for $l = 1$ **to** L **do**

Draw $(a_l, b_l) \sim \mu_1(\cdot \mid \tilde{\mathbf{n}})$ and $(a'_l, b'_l) \sim \mu_0(\cdot \mid \tilde{\mathbf{n}})$;

Set $d_l = |a_l - a'_l| + |b_l - b'_l|$;

end

Define $\widehat{\Delta}(\epsilon) = \frac{1}{L} \sum_{l=1}^L \tanh\left(\frac{\epsilon d_l}{2}\right)$;

Initialize $\epsilon_{\text{min}} = 0$ and choose ϵ_{max} such that $\widehat{\Delta}(\epsilon_{\text{max}}) \geq \tau$;

while $\epsilon_{\text{max}} - \epsilon_{\text{min}} > \text{tol}$ **do**

Set $\epsilon_{\text{mid}} = (\epsilon_{\text{min}} + \epsilon_{\text{max}}) / 2$;

Set $(\epsilon_{\text{min}}, \epsilon_{\text{max}}) \leftarrow \begin{cases} (\epsilon_{\text{mid}}, \epsilon_{\text{max}}), & \widehat{\Delta}(\epsilon_{\text{mid}}) < \tau, \\ (\epsilon_{\text{min}}, \epsilon_{\text{mid}}), & \text{otherwise.} \end{cases}$;

end

Set $\epsilon_{\text{lb}} = \epsilon_{\text{max}}$ and report ϵ_{lb} .

S.1.3 Algorithms for Frequentist-calibrated Decision Rules

The following two algorithms implement the frequentist-calibrated decision rules with type I error control described in Section 4.2 of the main text. Algorithm S.4 implements the worst-case calibration and Algorithm S.5 describes the data-adaptive calibration.

Algorithm S.4: Worst-case Calibration of the Threshold

Input: group sizes (n_1, n_0) ; significance level α ; type I error level α_{Freq} ; Monte Carlo size R ; privatized counts $\tilde{\mathbf{n}}$.

Output: threshold t_{LFC}^* and decision rule $\delta_{\text{LFC}}(\tilde{\mathbf{n}})$.

for $K = 0, 1, \dots, n$ **do**

for $r = 1$ **to** R **do**

 Draw $A_r \sim \text{Hypergeometric}(n, K, n_1)$ and set $(a_{11}^{(r)}, b_{01}^{(r)}) = (A_r, K - A_r)$;

 Run DP-FRT-Bayes on $(a_{11}^{(r)}, b_{01}^{(r)})$ to obtain $(\tilde{a}_{11}^{(r)}, \tilde{b}_{01}^{(r)})$;

 Compute $\psi^{(r)} = \Pr(p_{\text{FRT}} \leq \alpha \mid \tilde{a}_{11}^{(r)}, \tilde{b}_{01}^{(r)})$;

end

 Compute t_K as the empirical $(1 - \alpha_{\text{Freq}})$ -quantile of $\{\psi^{(r)}\}_{r=1}^R$;

end

Set $t_{\text{LFC}}^* = \max_K t_K$ and report decision $\delta_{\text{LFC}} = \mathbf{1}(\Pr(p_{\text{FRT}} \leq \alpha \mid \tilde{\mathbf{n}}) > t_{\text{LFC}}^*)$.

Algorithm S.5: Data-adaptive Calibration of the Threshold

Input: group sizes (n_1, n_0) ; significance level α ; type I error level α_{Freq} ; Monte Carlo size R ; confidence level $\zeta < \alpha_{\text{Freq}}$; privatized counts $\tilde{\mathbf{n}}$.

Output: threshold $t_{\text{Neyman}}^*(\tilde{\mathbf{n}})$ and decision $\delta_{\text{Neyman}}(\tilde{\mathbf{n}})$.

for $K = 0, 1, \dots, n$ **do**

for $r = 1$ **to** R **do**

 Draw $A_r \sim \text{Hypergeometric}(n, K, n_1)$ and set $(a_{11}^{(r)}, b_{01}^{(r)}) = (A_r, K - A_r)$;

 Run DP-FRT-Bayes to obtain $(\tilde{a}_{11}^{(r)}, \tilde{b}_{01}^{(r)})$;

 Compute $\psi^{(r)} = \Pr(p_{\text{FRT}} \leq \alpha \mid \tilde{a}_{11}^{(r)}, \tilde{b}_{01}^{(r)})$;

end

 Use the empirical distribution of $\{(\tilde{a}_{11}^{(r)}, \tilde{b}_{01}^{(r)})\}_{r=1}^R$ to approximate Q_K ;

 Form the smallest high-probability set A_K with mass at least $1 - \zeta$;

 Compute t'_K as the empirical $(1 - \alpha')$ -quantile of $\{\psi^{(r)}\}_{r=1}^R$, where $\alpha' = \alpha_{\text{Freq}} - \zeta$;

end

Define $C_{1-\zeta}(\tilde{\mathbf{n}}) = \{K : \tilde{\mathbf{n}} \in A_K\}$. Set $t_{\text{Neyman}}^*(\tilde{\mathbf{n}}) = \max_{K \in C_{1-\zeta}(\tilde{\mathbf{n}})} t'_K$ and report

$\delta_{\text{Neyman}}(\tilde{\mathbf{n}}) = \mathbf{1}(\Pr(p_{\text{FRT}} \leq \alpha \mid \tilde{\mathbf{n}}) > t_{\text{Neyman}}^*(\tilde{\mathbf{n}}))$.

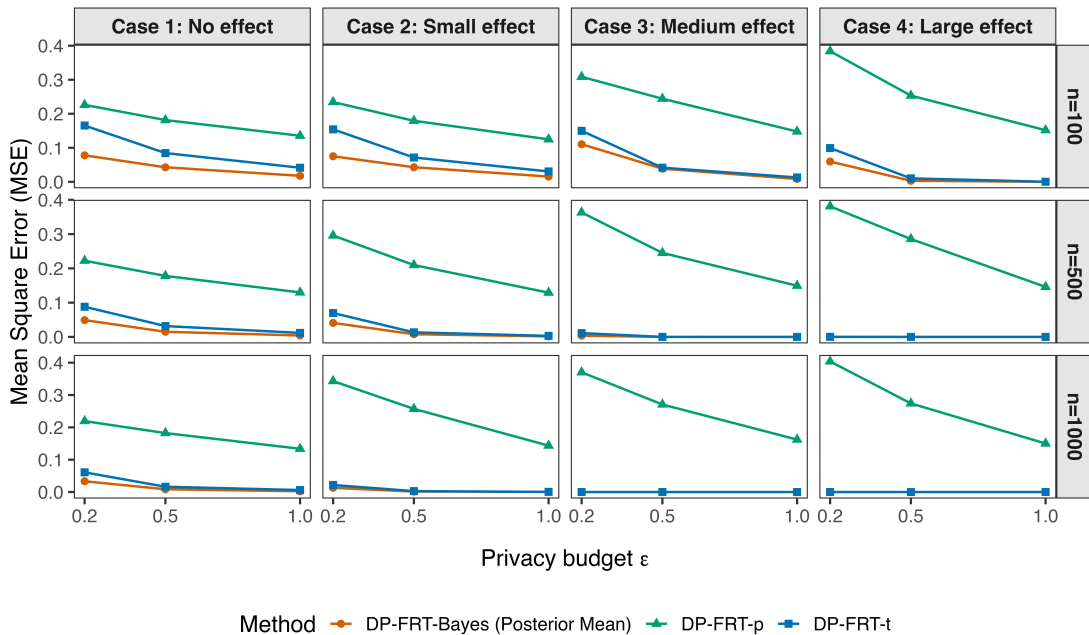


Figure S.1: MSE of different DP-FRT point estimators of p -values in Cases 1–4 when $\epsilon \in \{0.2, 0.5, 1\}$ and $n \in \{100, 500, 1000\}$.

S.2 Additional Simulation Studies

S.2.1 Additional Simulations for Estimating FRT p -value

We provide additional simulation results that complement Section 5.1 of the main text. They focus on the point estimation accuracy of several DP-FRT estimators. We use the same simulation design as in the main text.

Figure S.1 displays the MSE of three DP-FRT point estimators for the FRT p -value: DP-FRT-Bayes (posterior mean), DP-FRT-p, and DP-FRT-t. We find that DP-FRT-Bayes consistently achieves the smallest MSE, particularly when ϵ is small or the sample size is limited. The direct perturbation approaches DP-FRT-p and DP-FRT-t exhibit markedly larger MSE, with DP-FRT-p performing worst in most settings due to the high variability induced by directly perturbing the p -value. DP-FRT-t improves upon DP-FRT-p but still remains less efficient, and it offers no uncertainty quantification. These results demonstrate

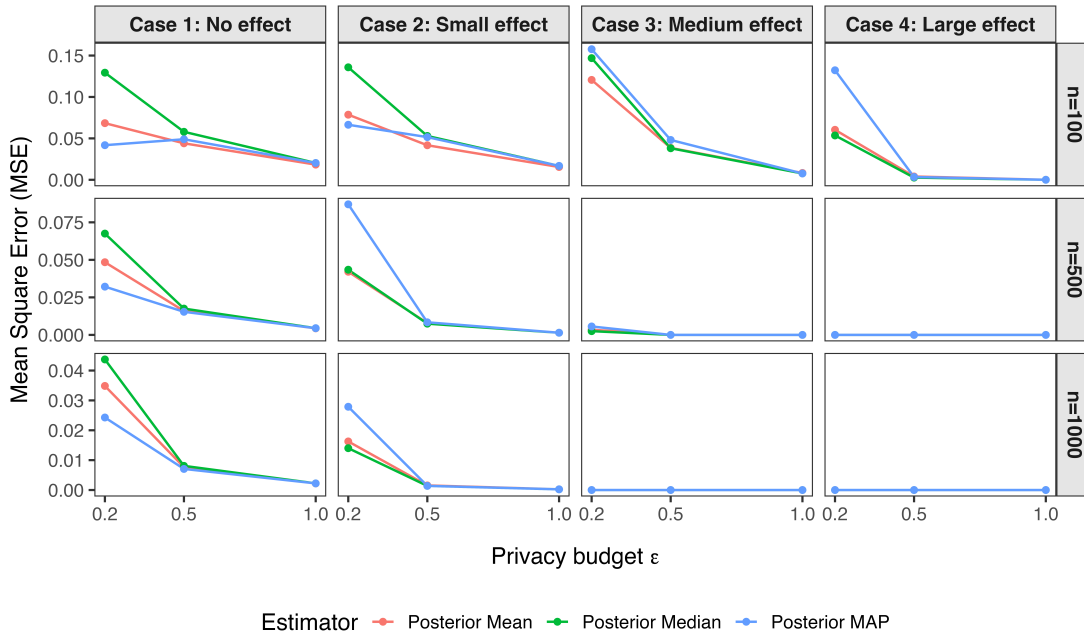
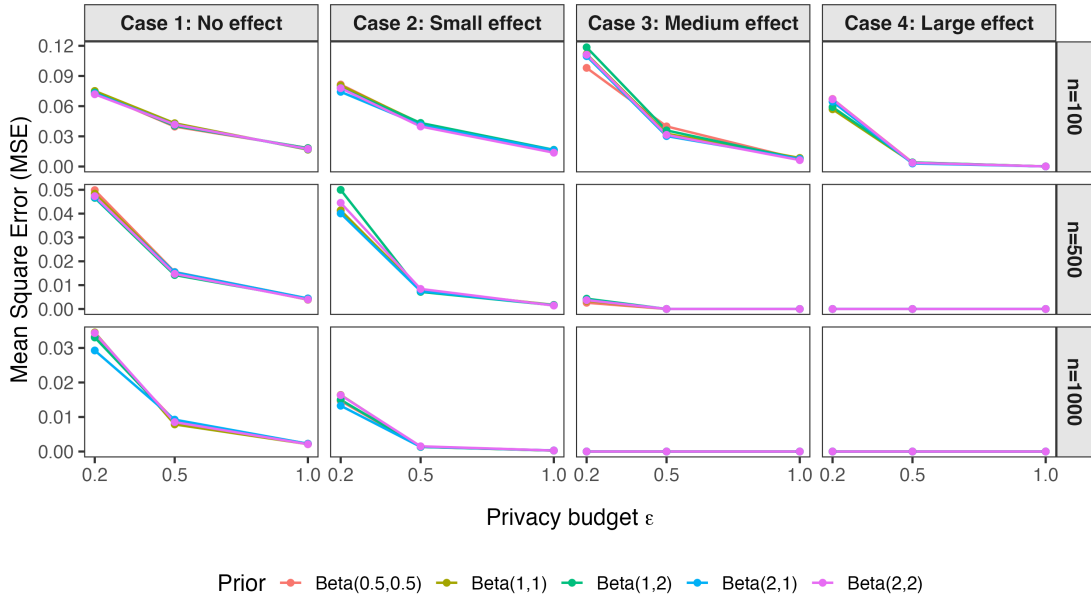


Figure S.2: MSE of different DP-FRT-Bayes point estimators of p -values in Cases 1–4 when $\epsilon \in \{0.2, 0.5, 1\}$ and $n \in \{100, 500, 1000\}$. The y-axis scales differ across panels.

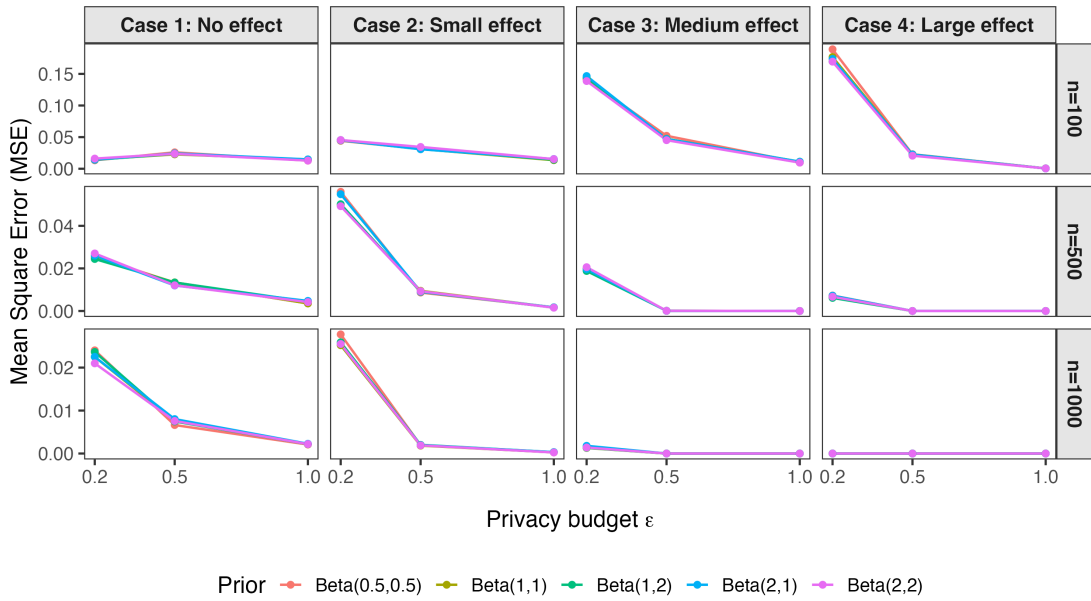
the clear advantage of DP-FRT-Bayes in stabilizing inference under DP.

Figure S.2 displays the MSE of different point estimators for the FRT p -value when using DP-FRT-Bayes. As expected, the MSE of all estimators decreases as either the privacy budget or sample size increases. Among the Bayesian methods, the posterior mean and posterior median achieve comparable MSE across most settings. The posterior MAP estimator occasionally exhibits larger MSE when ϵ is small, reflecting its sensitivity to multimodal posterior distributions induced by heavy DP noise. We recommend using the posterior mean estimator for its overall stability and accuracy.

Figure S.3 examines the prior sensitivity of the DP-FRT-Bayes posterior mean estimator for p -values under both independent Beta-binomial priors, which is (8) in the main text, and common success rate Beta priors, which is (9) in the main text. Note that choosing Beta(1, 1) in the Beta-binomial priors reduces to the uniform prior in (7) in the main text.



(a) Beta-binomial Priors



(b) Common Success Rate Beta Priors

Figure S.3: Prior sensitivity of the DP-FRT-Bayes posterior mean estimator for FRT p -value under (a) independent Beta-binomial priors and (b) common success rate Beta priors for $\epsilon \in \{0.2, 0.5, 1\}$ and $n \in \{100, 500, 1000\}$ in Cases 1–4. The y-axis scales differ across panels.

Across all settings, the MSE curves for different priors are nearly indistinguishable, indicating that the Bayesian denoising framework is robust to the choice of these priors.

S.2.2 Additional Simulations for Evaluating Decision Rules

In this section, we present additional simulation results that complement Section 5.2 of the main text. For the Bayesian sequential decision procedure, we focus on how a second-stage DP release with additional budget reduces abstention. For the frequentist tests, we focus on type I error control under the sharp null and power behavior under alternatives with nonzero treatment effects.

Table S.1 and Table S.2 summarize the behavior of two-stage Bayesian sequential decision. The first-stage abstention rate reports how often the posterior evidence Ψ falls inside the abstention region A , and ϵ_{lb} is the average data-adaptive lower bound on the additional privacy budget required to have a substantial chance of leaving A . The remaining columns report the empirical escape probability after a second independent release, where the top-up budget is set to $\epsilon_{\text{plus}} \in \{1, 2, 5, 10\} \times \epsilon_{\text{lb}}$. Across both tables, the escape probability increases monotonically as ϵ_{plus} is scaled up, illustrating how additional privacy budget translates into sharper posterior evidence and fewer abstentions. The reported ϵ_{lb} varies with the underlying scenario and sample size, reflecting that the amount of extra privacy budget needed to exit A is data-adaptive and instance-specific rather than a fixed constant.

Figure S.4 shows the rejection rates of the frequentist-calibrated decision rules across privacy budgets and sample sizes. Both the worst-case calibration described in Section 4.2.1 and the data-adaptive calibration described in Section 4.2.2 control the type I error at the nominal level under the sharp null (Case 5). The rejection rates increase with larger effect sizes or sample sizes (Cases 6–8), and the data-adaptive calibration is slightly more powerful than the worst-case calibration, as illustrated in the main text.

Table S.1: First-stage abstention rates (%), average ϵ_{lb} with $\xi = 0.05$, and escape rates (%) after second release at $\epsilon_{\text{plus}} \in \{1, 2, 5, 10\} \times \epsilon_{\text{lb}}$ in Cases 5–8 with $\epsilon = 0.2$.

Case	Abstain	ϵ_{lb}	Escape $_{1\times}$	Escape $_{2\times}$	Escape $_{5\times}$	Escape $_{10\times}$
(a) $n = 100$						
5: No effect	87.6	0.074	0.1	5.4	41.7	72.4
6: Small effect	90.6	0.080	0.0	4.2	30.2	61.0
7: Medium effect	94.6	0.080	0.0	6.0	24.5	46.8
8: Large effect	93.2	0.087	0.0	4.5	23.9	43.8
(b) $n = 500$						
5: No effect	50.5	0.057	1.2	13.7	46.5	75.4
6: Small effect	75.3	0.074	1.3	4.4	39.8	66.6
7: Medium effect	75.6	0.070	1.9	11.1	34.4	61.4
8: Large effect	49.4	0.065	0.2	12.3	50.4	72.7
(c) $n = 1000$						
5: No effect	28.5	0.047	0.0	14.4	54.0	76.5
6: Small effect	79.5	0.078	0.3	7.8	46.9	63.5
7: Medium effect	45.8	0.056	1.5	10.9	50.9	69.2
8: Large effect	5.2	0.046	0.0	36.5	73.1	96.2

Table S.2: First-stage abstention rates (%), average ϵ_{lb} with $\xi = 0.05$, and escape rates (%) after second release using $\epsilon_{\text{plus}} \in \{1, 2, 5, 10\} \times \epsilon_{\text{lb}}$ in Cases 5–8 with $\epsilon = 0.5$.

Case	Abstain	ϵ_{lb}	Escape $_{1\times}$	Escape $_{2\times}$	Escape $_{5\times}$	Escape $_{10\times}$
(a) $n = 100$						
5: No effect	39.2	0.129	1.0	13.3	54.1	81.6
6: Small effect	56.3	0.138	0.9	12.6	51.2	71.4
7: Medium effect	73.0	0.149	1.4	6.6	46.0	68.9
8: Large effect	81.2	0.187	0.4	3.8	42.5	69.8
(b) $n = 500$						
5: No effect	17.5	0.154	1.1	9.7	52.0	81.7
6: Small effect	40.9	0.149	0.2	12.0	50.1	71.1
7: Medium effect	35.5	0.154	0.0	10.7	46.8	64.5
8: Large effect	20.3	0.139	2.5	19.7	36.0	70.9
(c) $n = 1000$						
5: No effect	10.8	0.142	0.0	8.3	49.1	80.6
6: Small effect	39.8	0.175	1.5	7.8	44.5	74.9
7: Medium effect	12.5	0.170	0.0	11.2	54.4	80.8
8: Large effect	0.0	–	–	–	–	–

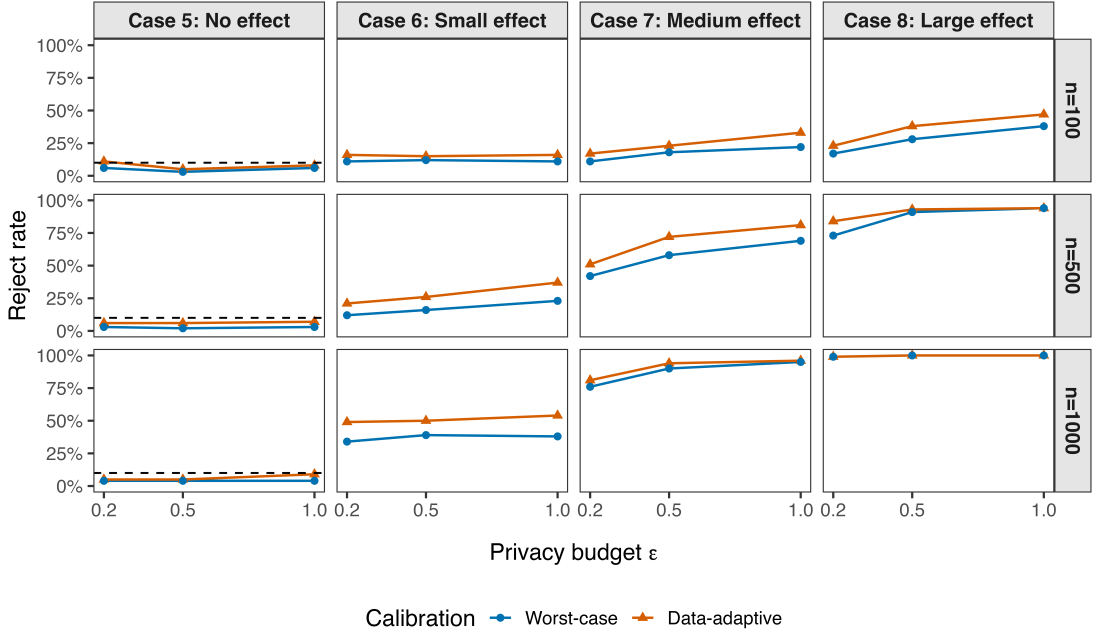


Figure S.4: Rejection rates of the frequentist-calibrated rules for $\epsilon \in \{0.2, 0.5, 1\}$ in Cases 5–8 under $n \in \{100, 500, 1000\}$. Horizontal black dashed line indicates the nominal type I error level $\alpha_{\text{Freq}} = 0.1$, while $\zeta = 0.01$ is used for the data-adaptive calibration method. Rates based on 100 simulation runs.

S.3 Lemmas Supporting Claims in Main Text

S.3.1 Clipping Invariance of the Posterior

In Section 3.2 of the main text, we claim that posterior inferences in DP-FRT-Bayes are identical regardless of whether or not the DP counts are clipped. This fact eliminates the need for post-processing to enforce feasible ranges on privatized counts. To be more specific, the geometric mechanism can result in privatized counts \tilde{n}_{11} and \tilde{n}_{01} that fall outside the intervals $[0, n_1]$ or $[0, n_0]$, respectively. Lemma S.3.1 shows that it is not necessary to truncate these noisy counts to the feasible range of the true counts if one uses DP-FRT-Bayes for posterior inference. The posterior distribution remains unchanged when the released counts are clipped under the geometric mechanism.

Lemma S.3.1. *Let $n \in \{0, \dots, T\}$ denote a true count, and let $\tilde{n} = n + \eta$ be generated from the geometric mechanism. Let m be a random variable used for inferences about the unknown n with prior distribution $\{\pi_t\}_{t=0}^T$ on $\{0, \dots, T\}$. The likelihood function is $\tilde{n} \mid (m = t) \sim K(\cdot \mid t)$ with $K(\tilde{n} \mid t) = \kappa_\rho(|\tilde{n} - t|)$, where κ_ρ is multiplicatively separable: $\kappa_\rho(a + b) = \kappa_\rho(a)\kappa_\rho(b)/\kappa_\rho(0)$. Define $\tilde{n}^{\text{clip}} = \min(\max(\tilde{n}, 0), T)$. Then, for all $k \in \{0, \dots, T\}$,*

$$\Pr(m = k \mid \tilde{n}) = \Pr(m = k \mid \tilde{n}^{\text{clip}}). \quad (\text{S.3.1})$$

Proof. By Bayes' rule, for any $k \in \{0, \dots, T\}$ and any realized value $\tilde{n} = x$,

$$\Pr(m = k \mid \tilde{n} = x) = \frac{\pi_k \kappa_\rho(|k - x|)}{\sum_{t=0}^T \pi_t \kappa_\rho(|t - x|)}. \quad (\text{S.3.2})$$

If $x \in [0, T]$ there is nothing to prove. If $x < 0$, then for all $k \in \{0, \dots, T\}$, $|k - x| = |k - 0| + |0 - x|$. Hence, by multiplicative separability, we have

$$\kappa_\rho(|k - x|) = \frac{\kappa_\rho(|k - 0|) \kappa_\rho(|0 - x|)}{\kappa_\rho(0)}. \quad (\text{S.3.3})$$

Substituting this into the Bayes formula shows that the factor $\kappa_\rho(|0 - x|)/\kappa_\rho(0)$ cancels between numerator and denominator, yielding

$$\Pr(m = k \mid \tilde{n} = x) = \frac{\pi_k \kappa_\rho(|k - 0|)}{\sum_{t=0}^T \pi_t \kappa_\rho(|t - 0|)} = \Pr(m = k \mid \tilde{n}^{\text{clip}} = 0). \quad (\text{S.3.4})$$

If $x > T$, then for all $k \in \{0, \dots, T\}$ we have $|k - x| = |T - k| + |x - T|$, and the same argument gives

$$\Pr(m = k \mid \tilde{n} = x) = \frac{\pi_k \kappa_\rho(|T - k|)}{\sum_{t=0}^T \pi_t \kappa_\rho(|T - t|)} = \Pr(m = k \mid \tilde{n}^{\text{clip}} = T). \quad (\text{S.3.5})$$

Thus, $\Pr(m = k \mid \tilde{n}) = \Pr(m = k \mid \tilde{n}^{\text{clip}})$ in all cases. \square

The argument applies coordinate-wise for (n_{11}, n_{01}) , because the kernel is multiplicatively separable and the joint kernel factorizes across coordinates.

S.3.2 Escape from the Abstention Region

In Section 4.1.2 of the main text, we state that, conditional on $\Psi \in A$ where A is the abstention region, the probability of remaining in the abstention region after the top-up release decays exponentially fast in the additional privacy budget ϵ_{plus} . Intuitively, as $\epsilon_{\text{plus}} \rightarrow \infty$, the second-stage geometric release reveals the true cell counts with probability tending to one. Consequently, the refined posterior evidence Ψ^+ concentrates on the non-private decision $\mathbf{1}(p_{\text{FRT}} \leq \alpha)$. Lemma S.3.2 formalizes this exponential escape guarantee.

Lemma S.3.2. *Let $\Psi = \text{Pr}(p_{\text{FRT}} \leq \alpha \mid \tilde{\mathbf{n}})$ and $\Psi^+ = \text{Pr}(p_{\text{FRT}} \leq \alpha \mid \tilde{\mathbf{n}}, \tilde{\mathbf{n}}^+)$. Let $A = (t_{\text{low}}, t_{\text{high}})$ be the abstention region with $0 < t_{\text{low}} < t_{\text{high}} < 1$. Assume $\text{Pr}(\Psi \in A) > 0$. There exists a finite constant $c > 0$ such that, for all $\epsilon_{\text{plus}} > 0$,*

$$\text{Pr}(\Psi^+ \notin A \mid \Psi \in A) \geq 1 - ce^{-\epsilon_{\text{plus}}}. \quad (\text{S.3.6})$$

Proof. The proof proceeds in three steps: (1) establishing posterior concentration on the true cell counts after the top-up release; (2) translating posterior concentration into escape from the abstention region; and, (3) converting the unconditional escape bound into the desired conditional probability bound.

In the first step, we analyze the posterior concentration around the true counts. Define the event $\mathcal{E} = \{\eta_{11}^+ = 0, \eta_{01}^+ = 0\}$. Since $\eta_{11}^+, \eta_{01}^+ \stackrel{\text{i.i.d.}}{\sim} \text{Geom}(\rho^+)$, we have

$$\text{Pr}(\mathcal{E}^c) = 1 - \left(\frac{1 - \rho^+}{1 + \rho^+} \right)^2 = \frac{4\rho^+}{(1 + \rho^+)^2} \leq 4\rho^+. \quad (\text{S.3.7})$$

With \mathcal{E} , we have $\tilde{n}_{11}^+ = n_{11}$ and $\tilde{n}_{01}^+ = n_{01}$, so

$$\kappa_{\rho^+}(\tilde{n}_{11}^+ - a)\kappa_{\rho^+}(\tilde{n}_{01}^+ - b) = \kappa_{\rho^+}(n_{11} - a)\kappa_{\rho^+}(n_{01} - b). \quad (\text{S.3.8})$$

For $(a, b) = (n_{11}, n_{01})$ this factor equals $\kappa_{\rho^+}(0)\kappa_{\rho^+}(0)$, while for any $(a, b) \neq (n_{11}, n_{01})$ we have $|a - n_{11}| + |b - n_{01}| \geq 1$. Thus, we have

$$\kappa_{\rho^+}(n_{11} - a)\kappa_{\rho^+}(n_{01} - b) \leq \kappa_{\rho^+}(0)^2(\rho^+)^{|a - n_{11}| + |b - n_{01}|} \leq \kappa_{\rho^+}(0)^2\rho^+. \quad (\text{S.3.9})$$

Next, we control the remaining factors uniformly in $\tilde{\mathbf{n}}$. Let S denote the finite support of (m_{11}, m_{01}) , which are the random variables representing the unknown true counts in the analyst's inference. Because the prior is strictly positive on S , there exist constants $0 < \pi_{\min} \leq \pi(a, b) \leq \pi_{\max} < \infty$ for all $(a, b) \in S$. For any integers x and any $(a, b) \in S$,

$$\frac{\kappa_\rho(x - a)}{\kappa_\rho(x - n_{11})} = \rho^{|x-a|-|x-n_{11}|}, \quad (\text{S.3.10})$$

and by the triangle inequality, $||x - a| - |x - n_{11}|| \leq |a - n_{11}|$. Since $0 < \rho < 1$, this implies

$$\frac{\kappa_\rho(x - a)}{\kappa_\rho(x - n_{11})} \leq \rho^{-|a-n_{11}|}. \quad (\text{S.3.11})$$

Applying this to both coordinates, we obtain, for any $(a, b) \in S$,

$$\frac{\kappa_\rho(\tilde{n}_{11} - a)\kappa_\rho(\tilde{n}_{01} - b)}{\kappa_\rho(\tilde{n}_{11} - n_{11})\kappa_\rho(\tilde{n}_{01} - n_{01})} \leq \rho^{-|a-n_{11}|-|b-n_{01}|}, \quad (\text{S.3.12})$$

and hence

$$\frac{\pi(a, b)\kappa_\rho(\tilde{n}_{11} - a)\kappa_\rho(\tilde{n}_{01} - b)}{\pi(n_{11}, n_{01})\kappa_\rho(\tilde{n}_{11} - n_{11})\kappa_\rho(\tilde{n}_{01} - n_{01})} \leq \frac{\pi_{\max}}{\pi_{\min}} \rho^{-|a-n_{11}|-|b-n_{01}|}. \quad (\text{S.3.13})$$

Since S is finite, the right-hand side admits a finite maximum over $(a, b) \neq (n_{11}, n_{01})$. Thus there exists a finite constant $C_1 > 0$, depending only on the prior and ρ , such that for all $\tilde{\mathbf{n}}$ and all $(a, b) \neq (n_{11}, n_{01})$,

$$\frac{\pi(a, b)\kappa_\rho(\tilde{n}_{11} - a)\kappa_\rho(\tilde{n}_{01} - b)}{\pi(n_{11}, n_{01})\kappa_\rho(\tilde{n}_{11} - n_{11})\kappa_\rho(\tilde{n}_{01} - n_{01})} \leq C_1. \quad (\text{S.3.14})$$

Combining the bounds (S.3.9) and (S.3.14), we obtain that on \mathcal{E} ,

$$\frac{\gamma^+(a, b)}{\gamma^+(n_{11}, n_{01})} \leq C_1 \rho^+ \quad \text{for all } (a, b) \neq (n_{11}, n_{01}). \quad (\text{S.3.15})$$

Summing over all $(a, b) \neq (n_{11}, n_{01})$ in the finite support S gives

$$1 - \gamma^+(n_{11}, n_{01}) = \sum_{(a,b) \neq (n_{11}, n_{01})} \gamma^+(a, b) \leq C_2 \rho^+ \quad \text{on } \mathcal{E}, \quad (\text{S.3.16})$$

for some finite $C_2 > 0$ independent of $\tilde{\mathbf{n}}$ and ρ^+ . Notice that on \mathcal{E}^c we have the trivial bound $1 - \gamma^+(n_{11}, n_{01}) \leq 1$. Therefore,

$$1 - \gamma^+(n_{11}, n_{01}) \leq \mathbf{1}_{\mathcal{E}^c} + \mathbf{1}_{\mathcal{E}} C_2 \rho^+. \quad (\text{S.3.17})$$

Taking expectations and using $\Pr(\mathcal{E}^c) \leq 4\rho^+$ yields

$$\mathbb{E} \left(1 - \gamma^+(n_{11}, n_{01}) \right) \leq 4\rho^+ + C_2 \rho^+ \leq C \rho^+ = C e^{-\epsilon_{\text{plus}}}, \quad (\text{S.3.18})$$

for some finite constant $C > 0$ independent of ϵ_{plus} .

In the second step, we translate posterior concentration into abstention probability. Let $p_{\text{FRT}} = g(n_{11}, n_{01})$ be the non-private FRT p -value. Notice that the corresponding non-private decision $H = \mathbf{1}(g(n_{11}, n_{01}) \leq \alpha)$ is a deterministic function of (n_{11}, n_{01}) . Then, by the definition of Ψ^+ , we have

$$\Psi^+ = \sum_{a,b} \mathbf{1}(g(a,b) \leq \alpha) \gamma^+(a,b). \quad (\text{S.3.19})$$

If $H = 1$, then (n_{11}, n_{01}) is in the rejection region and

$$\Psi^+ = \gamma^+(n_{11}, n_{01}) + \sum_{\substack{(a,b) \neq (n_{11}, n_{01}) \\ g(a,b) \leq \alpha}} \gamma^+(a,b) \geq \gamma^+(n_{11}, n_{01}), \quad (\text{S.3.20})$$

hence

$$1 - \Psi^+ \leq 1 - \gamma^+(n_{11}, n_{01}). \quad (\text{S.3.21})$$

If $H = 0$, then (n_{11}, n_{01}) is in the acceptance region and

$$\Psi^+ = \sum_{\substack{(a,b) \neq (n_{11}, n_{01}) \\ g(a,b) \leq \alpha}} \gamma^+(a,b) \leq 1 - \gamma^+(n_{11}, n_{01}). \quad (\text{S.3.22})$$

Denote $d_A = \min\{t_{\text{low}}, 1 - t_{\text{high}}\} > 0$. If $1 - \gamma^+(n_{11}, n_{01}) \leq d_A$ and $H = 0$, then $\Psi^+ \leq d_A \leq t_{\text{low}}$, and thus $\Psi^+ \notin A$. If $1 - \gamma^+(n_{11}, n_{01}) \leq d_A$ and $H = 1$, then $1 - \Psi^+ \leq d_A \leq 1 - t_{\text{high}}$, so $\Psi^+ \geq t_{\text{high}}$ and hence $\Psi^+ \notin A$. Therefore, we have

$$\{\Psi^+ \in A\} \subseteq \{1 - \gamma^+(n_{11}, n_{01}) > d_A\}. \quad (\text{S.3.23})$$

Taking probabilities and applying Markov's inequality together with (S.3.18) gives

$$\begin{aligned} \Pr(\Psi^+ \in A) &\leq \Pr\left(1 - \gamma^+(n_{11}, n_{01}) > d_A\right) \\ &\leq \frac{\mathbb{E}(1 - \gamma^+(n_{11}, n_{01}))}{d_A} \\ &\leq \frac{C}{d_A} e^{-\epsilon_{\text{plus}}} = C_A e^{-\epsilon_{\text{plus}}}. \end{aligned} \tag{S.3.24}$$

In the final step, we derive the conditional escape probability that is of interest. By Bayes' rule,

$$\Pr(\Psi^+ \in A \mid \Psi \in A) = \frac{\Pr(\Psi^+ \in A, \Psi \in A)}{\Pr(\Psi \in A)} \leq \frac{\Pr(\Psi^+ \in A)}{\Pr(\Psi \in A)}. \tag{S.3.25}$$

Since Ψ depends only on the first release, $\Pr(\Psi \in A) = p_A > 0$ is a constant independent of ϵ_{plus} . Combining this with (S.3.24), we obtain

$$\Pr(\Psi^+ \in A \mid \Psi \in A) \leq \frac{C_A}{p_A} e^{-\epsilon_{\text{plus}}}. \tag{S.3.26}$$

Setting $c = C_A/p_A$ yields

$$\Pr(\Psi^+ \notin A \mid \Psi \in A) = 1 - \Pr(\Psi^+ \in A \mid \Psi \in A) \geq 1 - ce^{-\epsilon_{\text{plus}}}, \tag{S.3.27}$$

which completes the proof. □

S.4 Proofs for Theoretical Results in the Main Text

S.4.1 Proof of Lemma 3.1

We provide the proof of Lemma 3.1 in Section 3.1 of the main text, which derives the ℓ_1 -sensitivity of the FRT p -value under the CRE with binary outcomes.

Lemma 3.1. *Under the CRE with binary outcomes and the test statistic $\hat{\tau}$, the ℓ_1 -sensitivity of p_{FRT} is $\Delta_p = \max\{n_1/n, n_0/n\}$.*

Proof. Define $A(\mathbf{Z}) = \sum_{i=1}^n z_i Y_i^{\text{obs}}$ and $a = A(\mathbf{Z}^{\text{obs}})$. Since $n_{01}(\mathbf{Z}) = n_{+1} - A(\mathbf{Z})$, we have $\hat{\tau}(\mathbf{Z}; \mathbf{Y}^{\text{obs}}) = [(1/n_1) + (1/n_0)]A(\mathbf{Z}) - n_{+1}/n_0$; hence, $\hat{\tau}$ is strictly increasing in $A(\mathbf{Z})$. Therefore, $p_{\text{FRT}} = |\mathcal{Z}|^{-1} \sum_{\mathbf{Z} \in \mathcal{Z}} \mathbf{1}(A(\mathbf{Z}) \geq a)$.

Let D and D' differ only at unit j , and set $s = Y'_j - Y_j \in \{-1, +1\}$. Then for D' , $A'(\mathbf{Z}) = A(\mathbf{Z}) + sz_j$ and $a' = a + sz_j^{\text{obs}}$. If $z_j = z_j^{\text{obs}}$ the indicator is unchanged; if $z_j \neq z_j^{\text{obs}}$ it can change by at most one in absolute value. Averaging over \mathcal{Z} gives

$$|p_{\text{FRT}}(D) - p_{\text{FRT}}(D')| \leq \frac{1}{|\mathcal{Z}|} \sum_{\mathbf{Z} \in \mathcal{Z}} \mathbf{1}(z_j \neq z_j^{\text{obs}}) = \begin{cases} n_1/n, & z_j^{\text{obs}} = 0, \\ n_0/n, & z_j^{\text{obs}} = 1. \end{cases} \quad (\text{S.4.28})$$

Maximizing over j yields $\Delta_p \leq \max\{n_1/n, n_0/n\}$. Tightness holds in two extremal constructions. If all $Y_i^{\text{obs}} = 0$ and $z_j^{\text{obs}} = 1$, then $p_{\text{FRT}}(D) = 1$, while after flipping Y_j^{obs} to 1, we obtain $p_{\text{FRT}}(D') = \Pr(Z_j = 1) = n_1/n$. So the gap is n_0/n . Symmetrically, if all $Y_i^{\text{obs}} = 1$ and $z_j^{\text{obs}} = 0$, the gap is n_1/n . In particular, under the balanced design $n_1 = n_0 = n/2$, the sensitivity is $\Delta_p = 1/2$. \square

S.4.2 Proof of Lemma 3.3

We provide the proof of Lemma 3.3 in Section 3.1 of the main text, which computes the ℓ_1 -sensitivity of the test statistic $\hat{\tau}$ under the CRE with binary outcomes.

Lemma 3.3. *Under the CRE with binary outcomes, the ℓ_1 -sensitivity of $\hat{\tau}$ is $\Delta_{\hat{\tau}} = \max\{1/n_1, 1/n_0\}$.*

Proof. If $Z_j^{\text{obs}} = 1$, flipping Y_j^{obs} changes n_{11} by ± 1 and keeps n_{01} unchanged, so $\Delta_{\hat{\tau}} = 1/n_1$. If $Z_j^{\text{obs}} = 0$, it changes n_{01} by ± 1 and keeps n_{11} unchanged, so $\Delta_{\hat{\tau}} = 1/n_0$. Maximizing over j yields the claim. In a balanced design, $\Delta_{\hat{\tau}} = 2/n$. \square

S.4.3 Proof of Theorem 4.2

We provide the proof of Theorem 4.2 in Section 4.1.2 of the main text, which provides an upper bound on the probability of exiting the abstention region after the second release when spending an additional ϵ_{plus} of privacy budget.

Theorem 4.2. *Let $A = (t_{\text{low}}, t_{\text{high}})$ be the abstention region with $0 < t_{\text{low}} < t_{\text{high}} < 1$, and define $r(\Psi) = \min\{\Psi - t_{\text{low}}, t_{\text{high}} - \Psi\}$ whenever $\Psi \in A$. Then, for every $\epsilon_{\text{plus}} > 0$,*

$$\Pr(\Psi^+ \notin A \mid \Psi \in A) \leq 2 \mathbb{E} \left(\frac{\Psi(1-\Psi)}{r(\Psi)} \Delta(\tilde{\mathbf{n}}; \epsilon_{\text{plus}}) \mid \Psi \in A \right).$$

Proof. The proof proceeds in three steps: (1) a channel-based representation of posterior refinement; (2) bounding the channel's total variation contraction via DP; and (3) converting mean movement into an upper bound on the probability of exiting the abstention region. For simplicity, denote $H = \mathbf{1}(p_{\text{FRT}} \leq \alpha)$. All expectations and probabilities in this proof are taken with respect to the joint law of $(H, \tilde{\mathbf{n}}, \tilde{\mathbf{n}}^+)$.

In the first step, we formulate the binary-input channel given the first release. Fix a realization $\tilde{\mathbf{n}}$ and condition on this event. Under this conditional law, we have $\Psi(\tilde{\mathbf{n}}) = \Pr(H = 1 \mid \tilde{\mathbf{n}}) \in [0, 1]$. For $h \in \{0, 1\}$, define the conditional output distributions as

$$Q_h(\cdot) = \mathcal{L}(\tilde{\mathbf{n}}^+ \mid H = h, \tilde{\mathbf{n}}). \tag{S.4.29}$$

Thus, conditionally on $\tilde{\mathbf{n}}$, $(H, \tilde{\mathbf{n}}^+)$ is a binary-input channel with input prior $\Pr(H = 1) = \Psi(\tilde{\mathbf{n}})$ and output kernel $\{Q_0, Q_1\}$.

Let Y denote a generic random variable with distribution $\mathcal{L}(\tilde{\mathbf{n}}^+ \mid \tilde{\mathbf{n}})$. Then, by Bayes' rule, the refined posterior can be written as $\Psi^+(Y) = \Pr(H = 1 \mid \tilde{\mathbf{n}}, Y)$. Conditionally on $\tilde{\mathbf{n}}$, one can compute

$$\mathbb{E}(|\Psi^+ - \Psi| \mid \tilde{\mathbf{n}}) = 2\Psi(1-\Psi)\text{TV}(Q_1, Q_0), \tag{S.4.30}$$

where $\text{TV}(\cdot, \cdot)$ denotes total variation distance.

In the second step, we bound $\text{TV}(Q_1, Q_0)$ via DP in a data-adaptive manner. Let $K(\cdot \mid a, b)$ denote the conditional law of the top-up release $\tilde{\mathbf{n}}^+$ given $(m_{11}, m_{01}) = (a, b)$, i.e., the geometric mechanism kernel. Conditionally on $\tilde{\mathbf{n}}$ and $H = h$, the posterior of the counts is supported on S_h and Q_h and is the corresponding mixture,

$$Q_h(\cdot) = \sum_{(a,b) \in S_h} K(\cdot \mid a, b) \Pr(m_{11} = a, m_{01} = b \mid H = h, \tilde{\mathbf{n}}), \quad h \in \{0, 1\}. \quad (\text{S.4.31})$$

Consider two arbitrary mixtures $Q_1 = \sum_i \alpha_i P_i$ and $Q_0 = \sum_j \beta_j R_j$ with weights summing to 1. By convexity of total variation, we have $\text{TV}(Q_1, Q_0) \leq \sum_{i,j} \alpha_i \beta_j \text{TV}(P_i, R_j)$. Applied here, writing $\mu_h(a, b) = \Pr(m_{11} = a, m_{01} = b \mid H = h, \tilde{\mathbf{n}})$ for $(a, b) \in S_h$, we obtain

$$\text{TV}(Q_1, Q_0) \leq \sum_{(a,b) \in S_1} \sum_{(a',b') \in S_0} \mu_1(a, b) \mu_0(a', b') \text{TV}(K(\cdot \mid a, b), K(\cdot \mid a', b')). \quad (\text{S.4.32})$$

The geometric mechanism on the counts has ℓ_1 -sensitivity equal to one and satisfies ϵ_{plus} -DP with respect to the adjacency $d((a, b), (a', b')) = 1$. By Ghazi & Issa (2024), we know that for an ϵ -DP mechanism K , any adjacent inputs z, z' obey

$$\text{TV}(K(\cdot \mid z), K(\cdot \mid z')) \leq s(\epsilon) = \tanh(\epsilon/2). \quad (\text{S.4.33})$$

Equip S with the ℓ_1 -metric $d((a, b), (a', b')) = |a - a'| + |b - b'|$. Then, by group privacy, for any two $(a, b), (a', b') \in S$, the mechanism satisfies $(d((a, b), (a', b')), \epsilon_{\text{plus}})$ -DP when viewed as a function of the input lattice point. Hence,

$$\text{TV}(K(\cdot \mid a, b), K(\cdot \mid a', b')) \leq s(d((a, b), (a', b'))) \epsilon_{\text{plus}}. \quad (\text{S.4.34})$$

Combining with (S.4.32), for each fixed $\tilde{\mathbf{n}}$, we obtain

$$\text{TV}(Q_1, Q_0) \leq \sum_{(a,b) \in S_1} \sum_{(a',b') \in S_0} \mu_1(a, b) \mu_0(a', b') s(\epsilon_{\text{plus}} d((a, b), (a', b'))) = \Delta(\tilde{\mathbf{n}}). \quad (\text{S.4.35})$$

Substituting (S.4.35) into (S.4.30), we obtain, for each fixed $\tilde{\mathbf{n}}$,

$$\mathbb{E}(|\Psi^+ - \Psi| \mid \tilde{\mathbf{n}}) \leq 2\Psi(1 - \Psi) \Delta(\tilde{\mathbf{n}}). \quad (\text{S.4.36})$$

In the final step, we establish how the mean movement translates into the abstention probability. Fix $\tilde{\mathbf{n}}$ such that $\Psi \in A$. The minimal distance from Ψ to the boundaries of A is $r(\Psi) = \min\{\Psi - t_{\text{low}}, t_{\text{high}} - \Psi\} > 0$. If $\Psi \in A$ and $\Psi^+ \notin A$, then necessarily $|\Psi^+ - \Psi| \geq r(\Psi)$, so

$$\{\Psi \in A, \Psi^+ \notin A\} \subseteq \{\Psi \in A, |\Psi^+ - \Psi| \geq r(\Psi)\}. \quad (\text{S.4.37})$$

Conditionally on this fixed $\tilde{\mathbf{n}}$ with $\Psi \in A$, we obtain

$$\Pr(\Psi^+ \notin A \mid \tilde{\mathbf{n}}) \leq \Pr(|\Psi^+ - \Psi| \geq r(\Psi) \mid \tilde{\mathbf{n}}). \quad (\text{S.4.38})$$

Applying Markov's inequality to the nonnegative random variable $|\Psi^+ - \Psi|$ yields

$$\Pr(|\Psi^+ - \Psi| \geq r(\Psi) \mid \tilde{\mathbf{n}}) \leq \frac{\mathbb{E}(|\Psi^+ - \Psi| \mid \tilde{\mathbf{n}})}{r(\Psi)}. \quad (\text{S.4.39})$$

Combining with (S.4.36) gives, for every $\tilde{\mathbf{n}}$ such that $\Psi \in A$,

$$\Pr(\Psi^+ \notin A \mid \tilde{\mathbf{n}}) \leq 2 \Delta(\tilde{\mathbf{n}}) \frac{\Psi(1 - \Psi)}{r(\Psi)}. \quad (\text{S.4.40})$$

Finally,

$$\Pr(\Psi^+ \notin A \mid \Psi \in A) = \mathbb{E}(\Pr(\Psi^+ \notin A \mid \tilde{\mathbf{n}}) \mid \Psi \in A). \quad (\text{S.4.41})$$

Using the bound from the previous step and the fact that Ψ , $r(\Psi)$, and $\Delta(\tilde{\mathbf{n}})$ are functions of $\tilde{\mathbf{n}}$, we obtain

$$\Pr(\Psi^+ \notin A \mid \Psi \in A) \leq 2 \mathbb{E} \left(\frac{\Psi(1 - \Psi)}{r(\Psi)} \Delta(\tilde{\mathbf{n}}) \mid \Psi \in A \right), \quad (\text{S.4.42})$$

which completes the proof. \square

S.4.4 Proof of Corollary 4.3

We provide the proof of Corollary 4.3 in Section 4.1.2 of the main text, which gives a data-adaptive necessary lower bound on the additional privacy budget ϵ_{plus} .

Corollary 4.3. *Let $A = (t_{\text{low}}, t_{\text{high}})$ be the abstention region with $0 < t_{\text{low}} < t_{\text{high}} < 1$. Fix a confidence level $1 - \xi \in (0, 1)$. For $\Psi \in A$, if the refined posterior Ψ^+ satisfies $\Pr(\Psi^+ \notin A \mid \tilde{\mathbf{n}}) \geq 1 - \xi$, then*

$$\epsilon_{\text{plus}} \geq \inf \left\{ \epsilon > 0 : \Delta(\tilde{\mathbf{n}}; \epsilon) \geq \frac{(1 - \xi) r(\Psi)}{2\Psi(1 - \Psi)} \right\},$$

where $r(\Psi) = \min\{\Psi - t_{\text{low}}, t_{\text{high}} - \Psi\}$, and $\Delta(\tilde{\mathbf{n}}; \epsilon)$ is defined as in Theorem 4.2.

Proof. From the proof of Theorem 4.2, for any fixed $\tilde{\mathbf{n}}$ with $\Psi \in A$,

$$\Pr(\Psi^+ \notin A \mid \tilde{\mathbf{n}}) \leq 2 \Delta(\tilde{\mathbf{n}}; \epsilon_{\text{plus}}) \frac{\Psi(1 - \Psi)}{r(\Psi)}. \quad (\text{S.4.43})$$

Assume that for some $\epsilon_{\text{plus}} > 0$ the desired bound $\Pr(\Psi^+ \notin A \mid \tilde{\mathbf{n}}) \geq 1 - \xi$ holds. Then,

$$1 - \xi \leq \Pr(\Psi^+ \notin A \mid \tilde{\mathbf{n}}) \leq 2 \Delta(\tilde{\mathbf{n}}; \epsilon_{\text{plus}}) \frac{\Psi(1 - \Psi)}{r(\Psi)}, \quad (\text{S.4.44})$$

which implies

$$\Delta(\tilde{\mathbf{n}}; \epsilon_{\text{plus}}) \geq \frac{(1 - \xi) r(\Psi)}{2\Psi(1 - \Psi)}. \quad (\text{S.4.45})$$

Since $s(x) = \tanh(x/2)$ is increasing on $[0, \infty)$ and satisfies $0 \leq s(x) < 1$, for any fixed $\tilde{\mathbf{n}}$ and any two values $0 \leq \epsilon_1 \leq \epsilon_2$ we have $s(\epsilon_1 d((a, b), (a', b'))) \leq s(\epsilon_2 d((a, b), (a', b')))$ for all $(a, b) \in S_1$ and $(a', b') \in S_0$. Multiplying by the nonnegative weights $\mu_1(a, b)\mu_0(a', b')$ and summing over $S_1 \times S_0$ yields $\Delta(\tilde{\mathbf{n}}; \epsilon_1) \leq \Delta(\tilde{\mathbf{n}}; \epsilon_2)$, so $\Delta(\tilde{\mathbf{n}}; \epsilon)$ is nondecreasing in ϵ .

Consequently, for any threshold $\tau \in (0, 1)$ the superlevel set $\{\epsilon > 0 : \Delta(\tilde{\mathbf{n}}; \epsilon) \geq \tau\}$ is of the form $[\epsilon^*, \infty)$ (possibly empty), where $\epsilon^* = \inf\{\epsilon > 0 : \Delta(\tilde{\mathbf{n}}; \epsilon) \geq \tau\}$. Taking $\tau = (1 - \xi) r(\Psi) (2\Psi(1 - \Psi))^{-1}$ completes the proof. \square

S.4.5 Proof of Theorem 4.4

We provide the proof of Theorem 4.4, which guarantees type I error control for the worst-case calibration procedure in Section 4.2.1 of the main text.

Theorem 4.4. *Under the sharp null H_0^F , we have $\Pr(\delta_{\text{LFC}}(\tilde{\mathbf{n}}) = 1) \leq \alpha_{\text{Freq}}$, where the probability averages over randomization and the privacy mechanism.*

Proof. Fix K , then by construction, we have

$$\Pr(\Pr(p_{\text{FRT}} \leq \alpha \mid \tilde{\mathbf{n}}) > t_K \mid K) \leq \alpha_{\text{Freq}}. \quad (\text{S.4.46})$$

Since $t_{\text{LFC}}^* \geq t_K$, it follows that

$$\Pr(\Pr(p_{\text{FRT}} \leq \alpha \mid \tilde{\mathbf{n}}) > t_{\text{LFC}}^* \mid K) \leq \alpha_{\text{Freq}}. \quad (\text{S.4.47})$$

Since this holds for every K , including the case where K equals the true total successes n_{+1} , the type I error is guaranteed to be no greater than α_{Freq} . \square

S.4.6 Proof of Theorem 4.6

We provide the proof of Theorem 4.6, establishing type I error control for the data-adaptive procedure described in Section 4.2.2 of the main text.

Theorem 4.6. *Fix $\zeta \in (0, \alpha_{\text{Freq}})$ and set $\alpha' = \alpha_{\text{Freq}} - \zeta$. Under the sharp null H_0^F , we have $\Pr(\delta_{\text{Neyman}}(\tilde{\mathbf{n}}) = 1) \leq \alpha_{\text{Freq}}$.*

Proof. Fix K and denote $\Psi = \Pr(p_{\text{FRT}} \leq \alpha \mid \tilde{\mathbf{n}})$. We first decompose

$$\begin{aligned} \Pr_K(\Psi > t_{\text{Neyman}}^*(\tilde{\mathbf{n}})) &= \Pr_K(\Psi > t_{\text{Neyman}}^*(\tilde{\mathbf{n}}), \tilde{\mathbf{n}} \in A_K) + \Pr_K(\Psi > t_{\text{Neyman}}^*(\tilde{\mathbf{n}}), \tilde{\mathbf{n}} \notin A_K) \\ &\leq \Pr_K(\Psi > t_{\text{Neyman}}^*(\tilde{\mathbf{n}}), \tilde{\mathbf{n}} \in A_K) + \Pr_K(\tilde{\mathbf{n}} \notin A_K). \end{aligned} \quad (\text{S.4.48})$$

On the event $\{\tilde{\mathbf{n}} \in A_K\}$ we have $K \in C_{1-\zeta}(\tilde{\mathbf{n}})$, so by the definition of $t_{\text{Neyman}}^*(\tilde{\mathbf{n}})$, $t_{\text{Neyman}}^*(\tilde{\mathbf{n}}) \geq t'_K$. Hence, $\{\Psi > t_{\text{Neyman}}^*(\tilde{\mathbf{n}})\} \subseteq \{\Psi > t'_K\}$ on $\{\tilde{\mathbf{n}} \in A_K\}$. Therefore,

$$\Pr_K(\Psi > t_{\text{Neyman}}^*(\tilde{\mathbf{n}}), \tilde{\mathbf{n}} \in A_K) \leq \Pr_K(\Psi > t'_K) \leq \alpha'. \quad (\text{S.4.49})$$

By Lemma 4.5 in the main text, we have $\Pr_K(\tilde{\mathbf{n}} \notin A_K) \leq \zeta$. Combining the two bounds gives

$$\Pr_K\left(\Psi > t_{\text{Neyman}}^*(\tilde{\mathbf{n}})\right) \leq \alpha' + \zeta = \alpha_{\text{Freq}}. \quad (\text{S.4.50})$$

Since this holds for every K , including the case where K equals the true total successes n_{+1} , the type I error is bounded by α_{Freq} . \square